



Sulfur-Based Denitrification in Streambank Subsoils in a Headwater Catchment Underlain by Marine Sedimentary Rocks in Akita, Japan

Atsushi Hayakawa^{1*}, Hitoshi Ota¹, Ryoki Asano², Hirotsu Murano³, Yuichi Ishikawa¹ and Tadashi Takahashi¹

¹Department of Biological Environment, Faculty of Bioresource Sciences, Akita Prefectural University, Akita, Japan, ²Department of Agro-Food Science, Faculty of Agro-Food Science, Niigata Agro-Food University, Tainai, Japan, ³Department of Environmental Bioscience, Faculty of Agriculture, Meijo University, Nagoya, Japan

OPEN ACCESS

Edited by:

Muhammad Shaaban,
Bahauddin Zakariya University,
Pakistan

Reviewed by:

Fan Chen,
Harbin Institute of Technology, China
Xiangyu Xu,
Hubei Academy of Agricultural
Sciences, China

*Correspondence:

Atsushi Hayakawa
hayakawa@akita-pu.ac.jp

Specialty section:

This article was submitted to
Biogeochemical Dynamics,
a section of the journal
Frontiers in Environmental Science

Received: 05 February 2021

Accepted: 23 August 2021

Published: 07 September 2021

Citation:

Hayakawa A, Ota H, Asano R,
Murano H, Ishikawa Y and Takahashi T
(2021) Sulfur-Based Denitrification in
Streambank Subsoils in a Headwater
Catchment Underlain by Marine
Sedimentary Rocks in Akita, Japan.
Front. Environ. Sci. 9:664488.
doi: 10.3389/fenvs.2021.664488

Sulfur-based denitrification may be a key biogeochemical nitrate (NO_3^-) removal process in sulfide-rich regions, but it is still poorly understood in natural terrestrial ecosystems. We examined sulfur-driven NO_3^- reduction using streambank soils in a headwater catchment underlain by marine sedimentary rock in Akita, Japan. In a catchment exhibiting higher sulfide content in streambed sediment, we sampled two adjacent streambank soils of streambank I (two layers) and of streambank II (eight layers). Anaerobic long-term incubation experiments (40 days, using soils of streambank I) and short-term incubation experiments (5 days, using soils of streambank II) were conducted to evaluate variations of N solutes (NO_3^- , NO_2^- , and NH_4^+), N gases (NO , N_2O), and the bacterial flora. In both experiments, two treatment solutions containing NO_3^- (N treatment), and NO_3^- and $\text{S}_2\text{O}_3^{2-}$ (N + S treatment) were prepared. In the N + S treatment of the long-term experiment, NO_3^- concentrations gradually decreased by 98%, with increases in the SO_4^{2-} , NO_2^- , NO , and N_2O concentrations and with not increase in the NH_4^+ , indicating denitrification had occurred with a high probability. Temporal accumulation of NO_2^- was observed in the N + S treatment. The stoichiometric ratio of SO_4^{2-} production and NO_3^- depletion rates indicated that denitrification using reduced sulfur occurred even without additional S, indicating inherent S also served as an electron donor for denitrification. In the short-term incubation experiment, S addition was significantly decreased NO_3^- concentrations and increased NO_2^- , NO , and N_2O concentrations, especially in some subsoils with higher sulfide contents. Many denitrifying sulfur-oxidizing bacteria (*Thiobacillus denitrificans* and *Sulfuricella denitrificans*) were detected in both streambank I and II, which dominated up to 5% of the entire microbial population, suggesting that these bacteria are widespread in sulfide-rich soil layers in the catchment. We concluded that the catchment with abundant sulfides in the subsoil possessed the potential for sulfur-driven NO_3^- reduction, which could widely influence N cycling in and NO_3^- export from the headwater catchment.

Keywords: sulfur-oxidizing bacteria, ecosystem denitrification, nitrogen cycle, biogeochemistry, sulfur-based denitrification

INTRODUCTION

Human activities have dramatically increased the amount of reactive nitrogen (N) in global ecosystems and have increased food production; however, input of reactive N beyond appropriate uses can lead to eutrophication of surface water, causing degradation of aquatic ecosystems and problems such as toxic algal blooms, loss of dissolved oxygen, depletion of fish populations, and biodiversity loss (Vitousek, 1997; Galloway and Cowling, 2002). In forest ecosystems, losses of N mainly as nitrate (NO_3^-) via streams can be caused by increased levels of reactive N such as N deposition in the forest (Lovett and Goodale, 2011). Denitrification is a NO_3^- removal process and is generally performed by particular groups of ubiquitous heterotrophic bacteria that have the ability to use NO_3^- as an electron acceptor and organic carbon (C) as an electron donor during anaerobic respiration. Denitrification transforms NO_3^- to the final form (N_2 gas) via four main steps: $\text{NO}_3^- \rightarrow \text{NO}_2^- \rightarrow \text{NO} \rightarrow \text{N}_2\text{O} \rightarrow \text{N}_2$ (Tiedje, 1994). Because denitrification ultimately removes reactive N as N_2 gas from the ecosystem as one of soil functions of transforming nutrients (Adhikari and Hartemink, 2016; Lilburne et al., 2020), it is a highly valued ecosystem service in N-enriched catchments (Craig et al., 2010).

Some bacteria can use inorganic sources, such as reduced sulfur compounds and Fe^{2+} , as the electron donor to grow chemoautotrophically (Korom, 1992; Straub et al., 1996). The oxidation of such inorganic species coupled with N oxide reduction is termed autotrophic denitrification. Autotrophic denitrification can proceed through the ability of some bacteria to couple the reduction of NO_3^- to the oxidation of reduced sulfur (Burgin and Hamilton, 2007). The most used electron donors of reduced sulfur compounds include elemental sulfur, sulfide and thiosulfate (De Capua et al., 2019). Some previous studies have detected NO_3^- removal coupled with sulfide oxidation in groundwater systems (Postma et al., 1991; Schwientek et al., 2008; Jørgensen et al., 2009; Craig et al., 2010; Vaclavkova et al., 2014), riverbed sediments (Hayakawa et al., 2013; Martínez-Santos et al., 2018; Yin et al., 2019), and sediment incubated with added sulfur (Brunet and Garcia-Gil, 1996; Garcia-Gil and Golterman, 1993; Jørgensen et al., 2009; Torrentó et al., 2010, 2011). NO_3^- reduction coupled with sulfide oxidation may be widespread and biogeochemically important in freshwater sediments (Burgin and Hamilton, 2008); however, the process has been reported less in freshwater than in marine and brackish marshes and tidal ecosystems (Hu et al., 2020) and the relative importance of the electron donor in the removal process remains uncertain at catchment scales.

Typical signs of sulfur-based denitrification using sulfide as an electron donor are decreasing NO_3^- accompanied by increasing SO_4^{2-} and NO_2^- (Postma et al., 1991; Jørgensen et al., 2009; Torrentó et al., 2010; Chung et al., 2014) and the microbial stoichiometric reaction ratios of SO_4^{2-} production and NO_3^- depletion rates ($\Delta\text{SO}_4^{2-}/\Delta\text{NO}_3^-$) for sulfur-based denitrification (Hayakawa et al., 2013; Vaclavkova et al., 2014). Some bioreactor studies have reported that NO_2^- accumulation was observed during sulfur-based denitrification (Moon et al., 2004; Chung

et al., 2014; Chen et al., 2018). Furthermore, a recent study has reported that accumulation of NO_2^- can also lead to build-up of NO and N_2O during the sulfur-based denitrification process (Lan et al., 2019). Microbial community analysis can provide useful information about the key players and complementary evidence of sulfur-based denitrification (Torrentó et al., 2011; Hayakawa et al., 2013; Dolejs et al., 2015; Wang et al., 2021). Therefore, to obtain evidence of sulfur-based denitrification in natural soils and sediments in freshwater ecosystems, it may be important to detect the various signs (NO_3^- reduction accompanied by SO_4^{2-} production, stoichiometric reactions inferred from the $\Delta\text{SO}_4^{2-}/\Delta\text{NO}_3^-$ ratio, accumulation of NO_2^- and gaseous forms of N, and elements of the microbial community) of sulfur-based denitrification.

The sulfur cycle is especially important in catchments that supply high concentrations of SO_4^{2-} to stream water (Szynkiewicz et al., 2012) and may be closely related to the N cycle through reactions such as sulfur-based denitrification in the catchments (Burgin and Hamilton, 2008). Reservoirs of sulfur in freshwater catchments are dominated by dissolved sulfate in water and sulfate and sulfide minerals in sediments and soils (Wynn et al., 2010; Iribar and Abalos, 2011; Hayakawa et al., 2020). In catchments supplying high levels of SO_4^{2-} to streams, it is expected to have much inherent sulfide. On one hand, the supplied SO_4^{2-} can be reduced to sulfide by the activity of dissimilatory sulfate-reducing bacteria in anoxic condition (Plugge et al., 2011), and the sulfide can be re-distributed to soils and sediments in the catchments. Reduction-oxidation reactions occur during burial because the sediments contain such reactive mixtures of oxidized and reduced components (Roberts, 2015). Some previous studies reported sulfide-driven autotrophic denitrification had occurred in sulfide-rich riverbed sediments in those catchments (Hayakawa et al., 2013; Martínez-Santos et al., 2018; Yin et al., 2019; Li et al., 2021).

Our study area, the Lake Hachiro watershed, is located along the coast of the Japan Sea, and its main surface geology consists of marine sedimentary rocks. The region was submerged beneath the sea during the Neogene Period (Shiraishi and Matoba, 1992), and sulfide minerals (easily oxidizable sulfur; EOS) in streambed sediments occur throughout the watershed, including in the forested area of the upper mountains, and may supply SO_4^{2-} to the streams from oxidation of sulfides (Hayakawa et al., 2020). High sulfide levels in streambed sediments can be reasonably expected to influence the N cycle through sulfur-based denitrification. Our previous study conducted in 35 headwater catchments in the Lake Hachiro watershed showed that in-stream NO_3^- concentrations tended to decrease with increasing EOS content in the streambed, indicating the probable occurrence of sulfur-based denitrification in the sulfide-rich catchment (Hayakawa et al., 2020). The composition of streambed sediment is affected by variations in the surface soil and geology of the catchment and has been used to identify sites with distinctive water quality (Horowitz and Elrick, 2017); thus, sulfide-rich soils are expected to be present somewhere in a catchment with a sulfide-rich streambed. In fact, soil with a high EOS content was found in a streambank

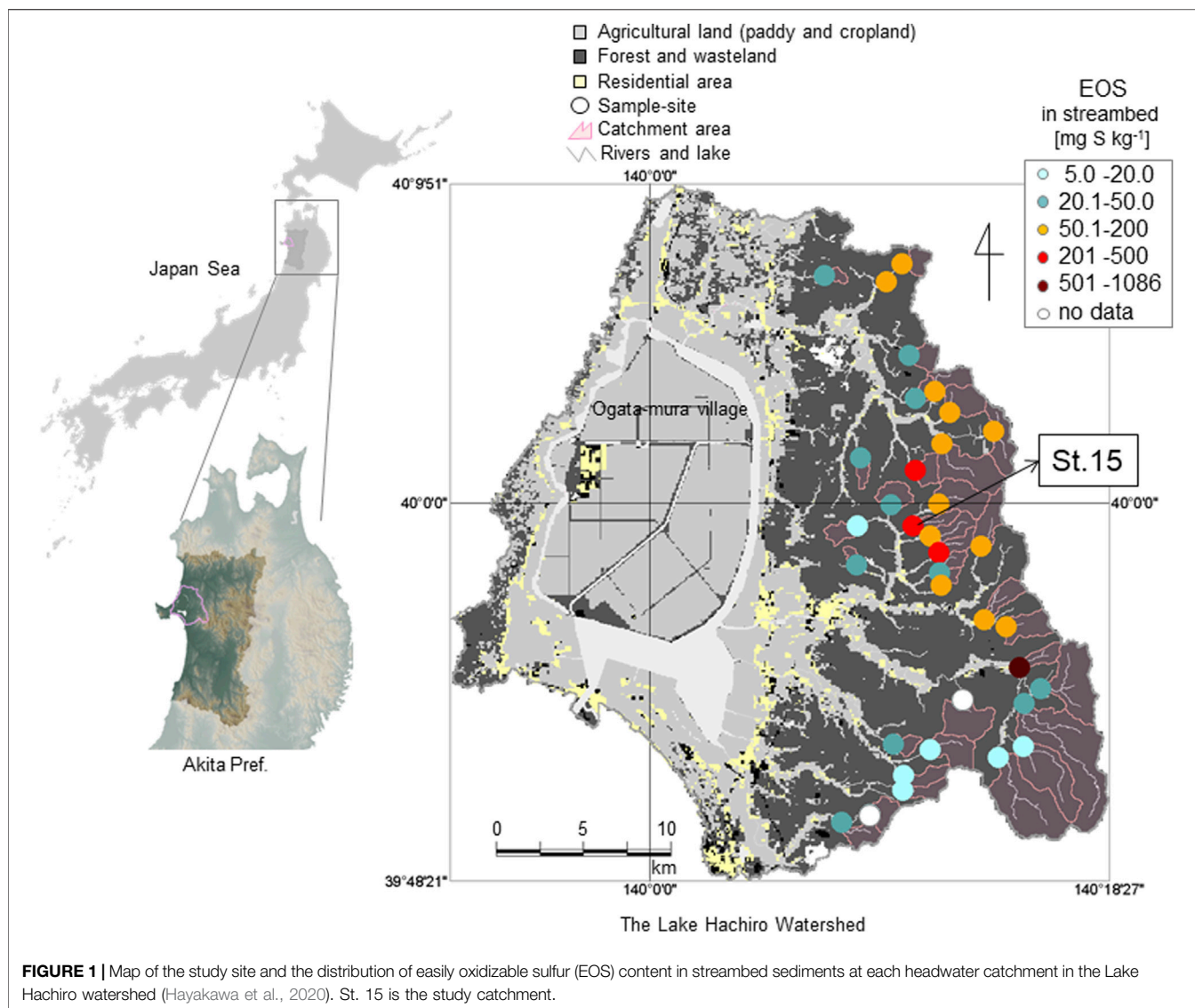


FIGURE 1 | Map of the study site and the distribution of easily oxidizable sulfur (EOS) content in streambed sediments at each headwater catchment in the Lake Hachiro watershed (Hayakawa et al., 2020). St. 15 is the study catchment.

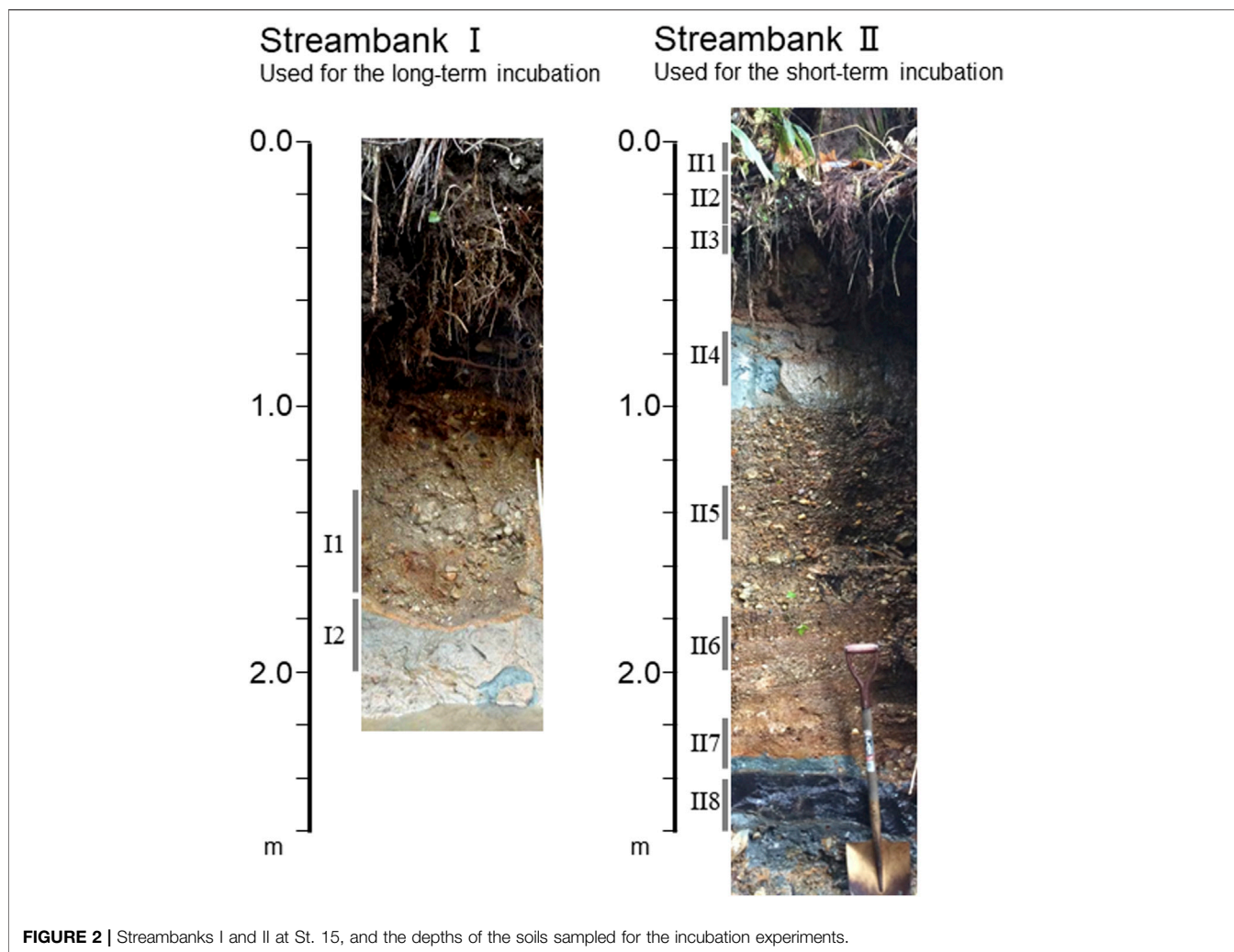
where the EOS content in the streambed was high (Hayakawa et al., 2020). To clarify this point, we need to obtain detailed evidence of sulfide distribution and potential sulfur-based denitrification in the natural soils in the Lake Hachiro watershed.

We hypothesized that the catchment with higher sulfide content in its streambed possesses sulfide-rich soil layers and a higher potential of sulfur-based denitrification in those layers within the catchment. We focused on streambank soils because these soils constitute an interface between land and stream, and thus can influence the qualities of the streambed sediment and stream. Our main study objectives were: 1) to evaluate the vertical distribution of sulfide in streambank soils; 2) to evaluate NO_3^- reduction with production of SO_4^{2-} , NO_2^- , NO , and N_2O in sulfide-rich soils and to detect signs of sulfur-based denitrification by anaerobic incubation with and without S addition; and 3) to identify the most important sulfur-oxidizing bacteria that cause denitrification.

MATERIALS AND METHODS

Site Description and Sediment Sampling

The Lake Hachiro watershed is located in western Akita Prefecture facing the Japan Sea (Figure 1). The entire watershed area is 894 km². The geological strata of the watershed belong to the Green Tuff zone, consisting of volcanic rocks and sedimentary rocks of late Miocene age (Shiraishi, 1990). In the early part of the middle Miocene to the Pliocene (i.e., ca 13–2.5 Ma), the Akita region was drowned as a result of subsidence of the former land area (Shiraishi and Matoba, 1992). As a result, the sedimentary rocks in the watershed are mainly marine deposits and consist of thick mudstone layers (Shiraishi, 1990) with high levels of total sulfur (0.90%; Koma, 1992). Weather recordings for the region from the Gojome recording station (8 km away from the study catchment) for the period 1981–2010 (Japan Meteorological Agency, 2013) revealed that average precipitation was



1,553 mm year⁻¹ and the annual mean temperature was 10.8°C. The lowest mean monthly temperature occurred in January (−0.9°C), and the highest mean monthly temperature was in August (24°C). The average maximum snow depth during winter (December–February) is 48 cm. Japanese cedar (*Cryptomeria japonica* D. Don) plantations dominated the forested area, especially in the middle and northern parts of the watershed.

The study catchment was St. 15 in the Lake Hachiro watershed (1.61 km², N39.9886, E140.1760), where the sulfide (EOS) content in streambed sediment is relatively high, as 0.254 g S kg⁻¹ (Hayakawa et al., 2020; **Figure 1**). In a recent study, the stream-water chemistry in the catchment exhibited the highest SO₄²⁻ (18.3 mg S L⁻¹) but relatively lower NO₃⁻ (0.149 mg N L⁻¹) concentrations among the 35 headwater catchments in the Lake Hachiro watershed (Hayakawa et al., 2020). Bulk N deposition to the catchment was 7.5 kg N ha⁻¹ year⁻¹ (Hayakawa et al., 2020), higher than the threshold value of 5 kg N ha⁻¹ yr⁻¹ that caused N leaching to streams in China (Fang et al., 2011).

Soil sampling was conducted at two streambanks, I and II, in St. 15 in April and May 2016, respectively (**Figure 2**). Streambank I is the right streambank, and was previously studied by

Hayakawa et al. (2020). Streambank II is the left bank approximately 50 m downstream from streambank I, and was newly exposed as the result of a recent flood (**Figure 2**). These streambanks might have been formed by flooding (not tidal in present) or mountain-side slope collapse, and the sediments accumulated in the streambanks may contain old and newly re-deposited reduced sulfur. Samples were collected by trowel at depths of 1.3–1.7 m (I1) and 1.7–2.0 m (I2) at streambank I for the evaluation of sulfur-based denitrification between the expected sulfide rich layer (I2) and the expected non-sulfide layer (I1). At streambank II, eight samples were collected at depths of 0–0.1 m (II1), 0.1–0.3 m (II2), 0.3–0.4 m (II3), 0.7–0.9 m (II4), 1.3–1.5 m (II5), 1.8–2.0 m (II6), 2.2–2.4 m (II7), and 2.4–2.6 m (II8). In roughly, soil textures were fine sands and silts in I2, II1, II2, II4, and II8, and were coarse sands with gravel in other layers. The bluish gray color of the soils in II2, II4, and II8 (**Figure 2**) indicated these sediments were formed under reducing conditions. To avoid contact with atmospheric oxygen, the sediments were taken by ca 15 cm depth from the streambank-wall surface and were sealed in sample bags for chemical analysis and incubation experiments and in 15 ml

centrifuge tubes for bacterial analysis immediately after sampling and stored in a cooler box with ice packs. Samples for the incubation and for measurement of the bacterial community were stored at 4°C and -80°C until analysis, respectively.

Incubation Procedure

The incubation method was based on previous studies (Jørgensen et al., 2009; Hayakawa et al., 2013). Long-term incubation of soil from streambank I (I1 and I2) was conducted to evaluate changes in the NO_3^- , NO_2^- , NO , and N_2O production/depletion patterns and the bacterial community. A 120 g quantity of fresh soil and 400 ml of solution were added to 550 ml glass bottles, which were then sealed with butyl rubber septa and an aluminum crimp. Two stainless-steel needles (Terumo, Tokyo, Japan, 23G \times 32 mm; GL Sciences, Tokyo, Japan, 19G \times 100 mm) were inserted into each septum and fitted with sterile three-way stopcocks for gas and solution sampling. Three treatment solutions were prepared: a deionized water control, CT; KNO_3 (8 mg N L^{-1}), N; and $\text{KNO}_3 + \text{Na}_2\text{S}_2\text{O}_3$ (20 mg S L^{-1}), N + S. Thiosulfate ($\text{S}_2\text{O}_3^{2-}$) is considered to be a useful electron donor for sulfur-based denitrification (Chung et al., 2014; Qian et al., 2016). To achieve anoxic conditions, the solution and headspace in the bottles were purged with O_2 -free ultrapure N_2 gas for 30 min. All bottles were prepared in triplicate and incubated at 25°C for 40 days in darkness. Because we intended to evaluate the potential of sulfur-based denitrification in the soils, the incubation was conducted in near the optimum growth temperature for sulfur denitrifying bacteria (e.g., *Thiobacillus denitrificans*, 28–32°C, Garrity et al., 2005).

Short-term incubation of soils from streambank II (II1–II8) was conducted to evaluate the vertical patterns of NO_3^- , NO_2^- , NO , and N_2O production/depletion and the bacterial community. The incubation procedure was almost same as that of the long-term incubation, but in a smaller bottle. A 15 g amount of fresh soil and 50 ml of solution were added to 150 ml glass bottles. Two treatment solutions were prepared: KNO_3 (5 mg N L^{-1}), N; and $\text{KNO}_3 + \text{Na}_2\text{S}_2\text{O}_3$ (10 mg S L^{-1}), N + S. All bottles were prepared in triplicate and incubated at 25°C for 5 days in darkness under anoxic conditions.

Water and Gas Sampling and Analysis

Water and gases in the incubation bottle were sampled eight times during the long-term incubation, at 1, 3, 6, 9, 14, 26, 30, and 40 days after the start of incubation, and twice during the short-term incubation, at 2 days (gas sample only) and 5 days after the start of incubation. In each sampling, 10- and 25 ml headspace gases in the bottle were sampled for the measurement of NO and N_2O , respectively. The NO concentration was measured immediately after the sampling by using a NO_x analyzer (MODEL42-i, Thermo Fisher Scientific, Yokohama, Japan). This analysis on the principle that NO and ozone (O_3) react to produce a characteristic luminescence with an intensity linearly proportional to the NO concentration. For N_2O analysis, the headspace gas was transferred from the syringe into a 15 ml evacuated glass vial and the N_2O concentration was determined using a gas chromatograph (GC14-B, Shimadzu, Kyoto, Japan) equipped with an electron-capture detector. For

water analysis, a 20 ml solution sample was extracted from the bottle with a 20 ml syringe. Immediately after the sampling, pH and electrical conductivity (EC) were measured in 5 ml of the sampled solution with a portable pH meter (B-212, HORIBA, Kyoto, Japan) and an EC meter (B-173, HORIBA, Kyoto, Japan). The remaining 15 ml of sampled solution was filtered through a 0.45 μm cellulose acetate membrane filter (DISMIC-13CP045AS, ADVANTEC, Tokyo, Japan). We measured the NO_2^- , NO_3^- , SO_4^{2-} , and $\text{S}_2\text{O}_3^{2-}$ concentrations in the solution using an ion chromatograph (DIONEX ICS-2100, Thermo Fisher Scientific, Yokohama, Japan). The detection limit for the analysis of $\text{S}_2\text{O}_3^{2-}$ concentration is 0.003 mg S L^{-1} . We determined the NH_4^+ concentration by colorimetry using the indophenol blue method with a continuous flow autoanalyzer (QuAAtro2-HR, BLTEC, Osaka, Japan). After every gas and water sampling, the same volume as the sampled gas and water of O_2 -free ultrapure N_2 gas was added to the bottle by using a syringe with a needle.

Soil Analysis

We determined the total C and total S contents in the sediments using the combustion method for C (SUMIGRAPH NC-22F, SCAS, Japan) and for S (LECO S632, Tokyo, Japan). Sediment pH (H_2O) and pH (H_2O_2) were determined by using soil/solution ratios of 1:2.5 (w/v) and 1:10 (w/v) (Murano et al., 2000), respectively. If the reduced sulfur are present in soils, they are often capable of rapid oxidation by H_2O_2 , causing lowered pH (H_2O_2) values. The easily oxidizable S (EOS) content in the soils was calculated as the difference between the H_2O_2 -soluble S content ($\text{H}_2\text{O}_2\text{-S}$) and the water-soluble S content ($\text{H}_2\text{O-S}$) (Murano et al., 2000). EOS represents reduced sulfur such as pyrite in sediments (Murano et al., 2000).

Analysis of Bacterial Communities in the Soil

To describe the bacterial communities in the streambank soils, 16S rRNA genes were analyzed by means of PCR pyrosequencing. Total DNA was extracted from 0.5 g soil using a FastDNA SPIN Kit for Soil (MP Biomedicals, Carlsbad, CA, United States) according to the manufacturer's instructions. DNA libraries were constructed based on two-step tailed PCR for 16S rRNA V4 region using primers (515f, 5'-GTGCCAGCMGCCGCGGTAA-3'; 806r, 5'-GGACTACHVGGGTWTCTAAT-3') with an Illumina nextera barcode (Caporaso et al., 2011, https://jp.support.illumina.com/downloads/16s_metagenomic_sequencing_library_preparation.html). The mixture for the amplification of the first step consisted of 1 \times KAPA HiFi HotStart Ready Mix (Roche, Basel, Switzerland), 0.25 μM of each primer, and 10 ng template DNA in a final volume of 25 μl . The amplification conditions were as follows: 94°C for 3 min; 25 cycles at 94°C for 60 s, 50°C for 60 s, and 72°C for 105 s; and a final extension at 72°C for 10 min. After purification on Agencourt AMPure XP (Beckman Coulter, Pasadena, CA, United States), second-step PCR was performed. The mixture for the amplification of the second step consisted of 1 \times KAPA HiFi HotStart Ready Mix, 0.25 μM of each primer, and 5 μl first-step PCR product in a final volume of 50 μl . After

purification on Agencourt AMPure XP, the concentrations were measured using a Qubit dsDNA BR Assay Kit (Thermo Fisher Scientific, Waltham, MA, United States). All PCR products were normalized to the same molecule concentration and mixed in equal volumes. The constructed libraries were subjected to 250-bp paired-end sequencing on an Illumina MiSeq with Miseq Reagent Kit v2 nano (500 Cycles).

Raw sequencing reads, which were divided into forward and reverse, were assembled using the Initial Process in the Ribosomal Database Project (RDP) Pyrosequencing Pipeline (<http://pyro.cme.msu.edu/>). Reads of 150 bp or fewer and those containing a sequence with a quality value of 20 or less were removed. Chimeric sequences were removed using Fungene chimera check Pipeline (<http://fungene.cme.msu.edu/>). Chimera-filtered sequences were classified phylogenetically using the RDP Classifier with a cut-off value of 0.8 (**Supplementary Figures S1, S2**). Sequences classified as belonging to sulfur-oxidizing bacteria were compared to sequences registered in the database of the DNA Databank of Japan by using the BLAST system (<http://blast.ddbj.nig.ac.jp/blast/blastn?lang=en>) to determine the most similar sequence type. In the sequences obtained in this study, sequences which exhibited more than 97% similarity to 16S rDNA sequences classified as SOB was considered. The nucleotide sequence data were deposited in the DDBJ Read Archive (http://trace.ddbj.nig.ac.jp/dra/index_e.html) under accession number DRA011495.

Data Analysis

For the evaluation of NO_3^- depletion and SO_4^{2-} production rates during incubation, the accumulated number of moles n (NO_3^- and SO_4^{2-}) of element i removed from or released to the solution over time up to sampling occasion k was calculated from the measured concentration (C_{meas}) following the method of Jørgensen et al. (2009) and Vaclavkova et al. (2014):

$$n_i^k = \left[C_{i,\text{meas}}^k V_{\text{total}}^k + \sum_{s=1}^k C_{i,\text{meas}}^s V_{\text{sample}}^s \right] (\text{moles})$$

where V_{total}^k is the total volume of solution in the bottle after removal of the k th sample and V_{sample}^s is the volume of sample removed on sampling occasion k . Elemental transformation rates were calculated using linear regression against time as the independent variable and concentration as the dependent variable. Average \pm standard deviation ($n = 3$) reaction rates (mmol per bottle) of NO_3^- depletion and SO_4^{2-} production were expressed as ΔNO_3^- and ΔSO_4^{2-} , respectively, and $\Delta\text{SO}_4^{2-}/\Delta\text{NO}_3^-$ was calculated.

The chimera-filtered sequences were divided into operational taxonomic units (OTUs) for sequences with over 97% similarity to one another by uclust method and furthest clustering algorithm using the Qiime 1.9.0 (<http://qiime.org/index.html>). Diversity indices, such as Chao1 and the abundance-based coverage estimate (ACE), were also calculated using Qiime (Chao and Bunge 2002) (**Supplementary Table S1**). Differences in microbial community structure among in the samples were calculated from OTUs by unweighted UniFrac using Qiime, and principal coordinate analysis was performed (**Supplementary Figure S3**).

One-way ANOVA was used followed by Bonferroni's test was used for multiple comparisons of variables among soils I1 and I2 in the long-term incubation. The Wilcoxon rank-sum test (U test) was used for comparisons between two treatments (N, N + S treatments). The Kruskal–Wallis test followed by the Steel–Dwass test were used for multiple comparisons of variables among soil layers I1 to I18, and bacterial communities among treatments in I2 during the long-term incubation. These statistical analyses were performed using R (R Development Core Team 2018; version 3.4.3).

RESULTS

Physio-Chemical Properties of Streambank Soils

The characteristics of the soils in the two streambanks are listed in **Table 1**. The pH (H_2O) was lowest in samples I2 (6.35) and I18 (5.54). The pH (H_2O_2) range was 3.04–7.08, with low values in I2, I11, I12, I14, and I18. EC was 2.9–726 mS m^{-1} , with high values in I2, I11, I14, and I18. Total carbon content was the highest (48 g kg^{-1}) in sample I11 of the surface soil. In contrast, high total sulfur contents were observed in subsoil samples I2, I14, and I18, and EOS levels were also high in those soil layers.

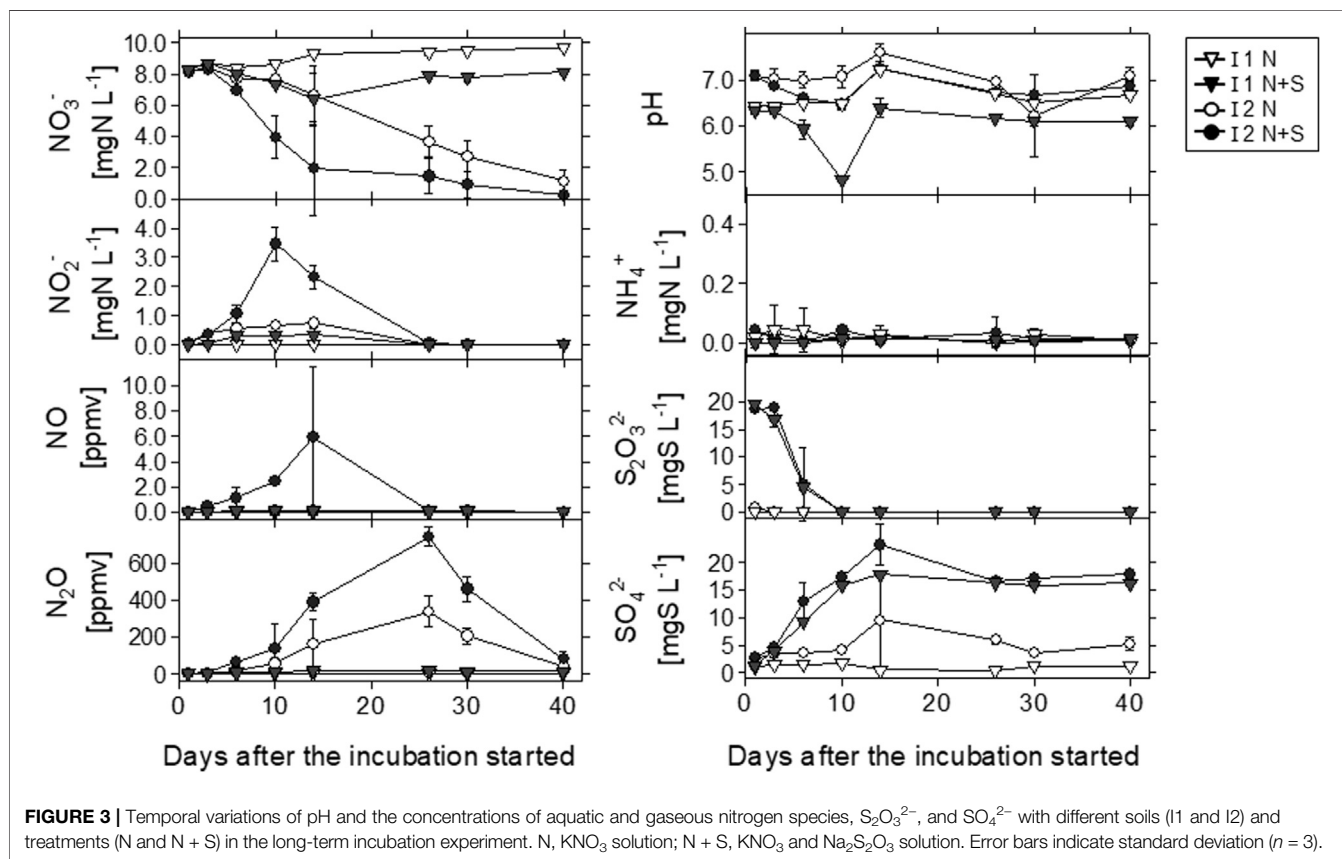
Long-Term Incubation Experiment

Temporal variations of the concentrations of aquatic and gaseous N species, $\text{S}_2\text{O}_3^{2-}$, and SO_4^{2-} in different soil layers (I1 and I2) and treatments (N and N + S) during the long-term incubation experiment are shown in **Figure 3**. NO_3^- concentrations decreased more with time in I2 than in I1, and in the N + S treatment than in the N treatment for each layer. On day 14 in I2, the NO_3^- concentration was markedly different between the N and N + S treatments, with values of 6.59 ± 1.7 and $1.94 \pm 3.0 \text{ mg N L}^{-1}$, respectively; the final values (on day 40) were 1.13 ± 0.73 and $0.22 \pm 0.20 \text{ mg N L}^{-1}$, respectively. In I2, the decrease in the NO_3^- concentration was followed by increases in the NO_2^- , NO, and N_2O concentrations. NO_2^- accumulation was particularly observed in the first 14 days, with levels increasing to 0.76 mg N L^{-1} in the N treatment and 3.46 mg N L^{-1} in the N + S treatment. In contrast, in I1, the NO_3^- concentration did not fall markedly, but decreased more in the N + S treatment than in the N treatment. NH_4^+ was detected, but at relatively low levels ($0.0\text{--}0.04 \text{ mg N L}^{-1}$), and exhibited no clear differences among soils and treatments.

The NO concentration increased in I2 with N + S treatment to a maximum value of 5.96 ppmv on day 14, but was almost undetectable in I1 with N treatment. N_2O was detected in both soils and treatments; the maximum values of 337 ppmv (N treatment) and 743 ppmv (N + S treatment) were observed in I2 on day 26. In I1 with N + S treatment, the maximum N_2O concentration was approximately 1/43 (17 ppmv) of that in I2 with N + S treatment. The N_2O concentration decreased rapidly after day 26, when NO_2^- and NO had almost disappeared. The $\text{S}_2\text{O}_3^{2-}$ concentration decreased rapidly in the first 10 days and was oxidized to SO_4^{2-} in both soils with N + S treatment. $\text{S}_2\text{O}_3^{2-}$ was detected at $0.83 \pm 0.02 \text{ mg S L}^{-1}$ on day 1 in I2 without S addition (N treatment) but was not detected in I1 with N treatment throughout the incubation period.

TABLE 1 | Soil chemical properties at streambanks I and II. EC, electric conductivity; T-C, total carbon; T-S, total sulfur; EOS, easily oxidizable sulfur.

Soil	depth, m	pH (H ₂ O)	pH (H ₂ O ₂)	EC	T-C	T-S	EOS
	M			mS m ⁻¹	g kg ⁻¹	g kg ⁻¹	g kg ⁻¹
I1	1.3–1.7	7.11	7.08	5.5	0.89	0.14	0.004
I2	1.7–2.0	6.35	4.58	69	3.6	1.7	1.2
II1	0.0–0.1	6.97	3.37	113	48	0.75	0.073
II2	0.1–0.3	7.39	5.14	5.1	2.3	0.15	0.017
II3	0.3–0.4	6.98	5.74	5.1	1.1	0.12	0.006
II4	0.7–0.9	6.90	5.41	89	3.0	1.2	0.33
II5	1.3–1.5	6.65	6.20	3.5	1.5	0.14	0.007
II6	1.8–2.0	7.41	6.22	2.9	0.7	0.12	0.006
II7	2.2–2.4	7.26	6.15	4.2	0.7	0.15	0.007
II8	2.4–2.6	5.54	3.04	726	5.9	96	4.9



The N + S treatment exhibited large fluctuations in water qualities and gas concentrations in sample I2 (**Figure 4**). By day 10, the NO₃⁻ concentration had fallen sharply, the NO₂⁻ concentration had increased, and the S₂O₃²⁻ concentration had decreased. During this interval, the pH fell from 7.1 to 6.5. After the NO₂⁻ peak on day 10, the maximum NO concentration was detected on day 14, at the same time as the pH increased to 7.2, followed by the N₂O peak concentration on day 26.

Using moles data in **Supplementary Figure S4**, the results of ΔNO_3^- and ΔSO_4^{2-} , and $\Delta\text{SO}_4^{2-}/\Delta\text{NO}_3^-$ during different incubation periods are shown in **Table 2**. Since NO₃⁻ and SO₄²⁻ were linearly changed especially during days 1–14 (**Supplementary**

Figure S4), we estimated ΔNO_3^- and ΔSO_4^{2-} values for days 1–14 and all the incubation period (1–40). In both the periods, ΔNO_3^- in I2 with N + S treatment was significantly larger than other treatments, and ΔSO_4^{2-} was significantly larger in the added S treatments (**Table 2**). On one hand, $\Delta\text{SO}_4^{2-}/\Delta\text{NO}_3^-$ did not differ between soils and treatments during days 1–14 and was significantly larger in I1 with N + S treatment during days 1–40 (**Table 2**). The relationships between ΔNO_3^- and ΔSO_4^{2-} of I1 and I2 with both treatments during different incubation periods showed that the results for I2 with N and N + S treatments plotted between the denitrification lines of S₂O₃²⁻ and FeS during days 1–14 with large variations (**Figure 5A**). During days 1–40, only I2 with N + S

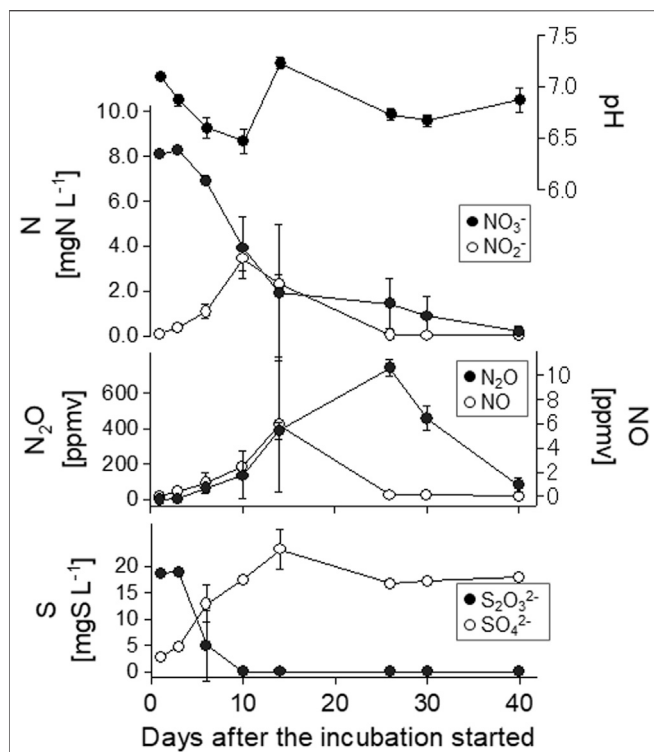


FIGURE 4 | Temporal variations of aquatic and gaseous nitrogen species and $S_2O_3^{2-}$ and SO_4^{2-} concentrations in I2 with N + S treatment in the long-term incubation experiment. N, KNO_3 solution; N + S, KNO_3 , and $Na_2S_2O_3$ solution. Error bars indicate standard deviation ($n = 3$).

treatment plotted between these lines with small variations (Figure 5B). In the case of I1, relatively larger ΔSO_4^{2-} than ΔNO_3^- resulted in higher $\Delta SO_4^{2-}/\Delta NO_3^-$ in the N + S treatment. In the N treatment of I1, both ΔNO_3^- and ΔSO_4^{2-} were small; therefore, these results plotted near zero.

Short-Term Incubation Experiment

The NO_3^- , NO_2^- , NO, and N_2O levels and the pH were compared among different treatments and soil layers in the short-term incubation experiment using soils II1–8 (Figures 6, 7, Table 3). Addition of S significantly decreased the NO_3^- concentration

($p < 0.01$) and pH ($p < 0.01$), and increased the NO_2^- ($p < 0.01$), NO ($p < 0.05$), and N_2O ($p < 0.05$) concentrations (Figure 6). These N species also changed markedly in the different soil layers (Figure 7, $p < 0.01$). NO_3^- concentrations in II4 and II8 tended to be lower, especially with added S (Table 3; Figure 7). The NO_2^- concentration rose with S addition in II4 (to 2.1 mg N L⁻¹) and II8 (to 0.57 mg N L⁻¹) (Table 3). SO_4^{2-} concentrations were higher in II4 (2.2 mg S L⁻¹) and II8 (10 mg S L⁻¹) without S addition (N treatment). $S_2O_3^{2-}$ was below the detection limit in any treatments or layers (data not shown). NO and N_2O concentrations after day 5 tended to be higher in II2, II4, and II8, especially with added S (Figure 7; Table 3). NO concentrations in II2, II4, and II8 with S addition increased to 12, 19, and 29 ppmv, respectively (Table 3); N_2O concentrations in II2, II4, and II8 with S addition increased to 84, 58, and 260 ppmv, respectively (Table 3). In II1, the NO_3^- concentration decreased to almost 0 mg N L⁻¹ in both treatments, and NO_2^- , NO, and N_2O were also almost undetectable after day 5, but NO and N_2O clearly increased after day 2 (Table 3). In II3, II5, II6, and II7, the decrease in NO_3^- and the increases in NO_2^- , NO, and N_2O were relatively small.

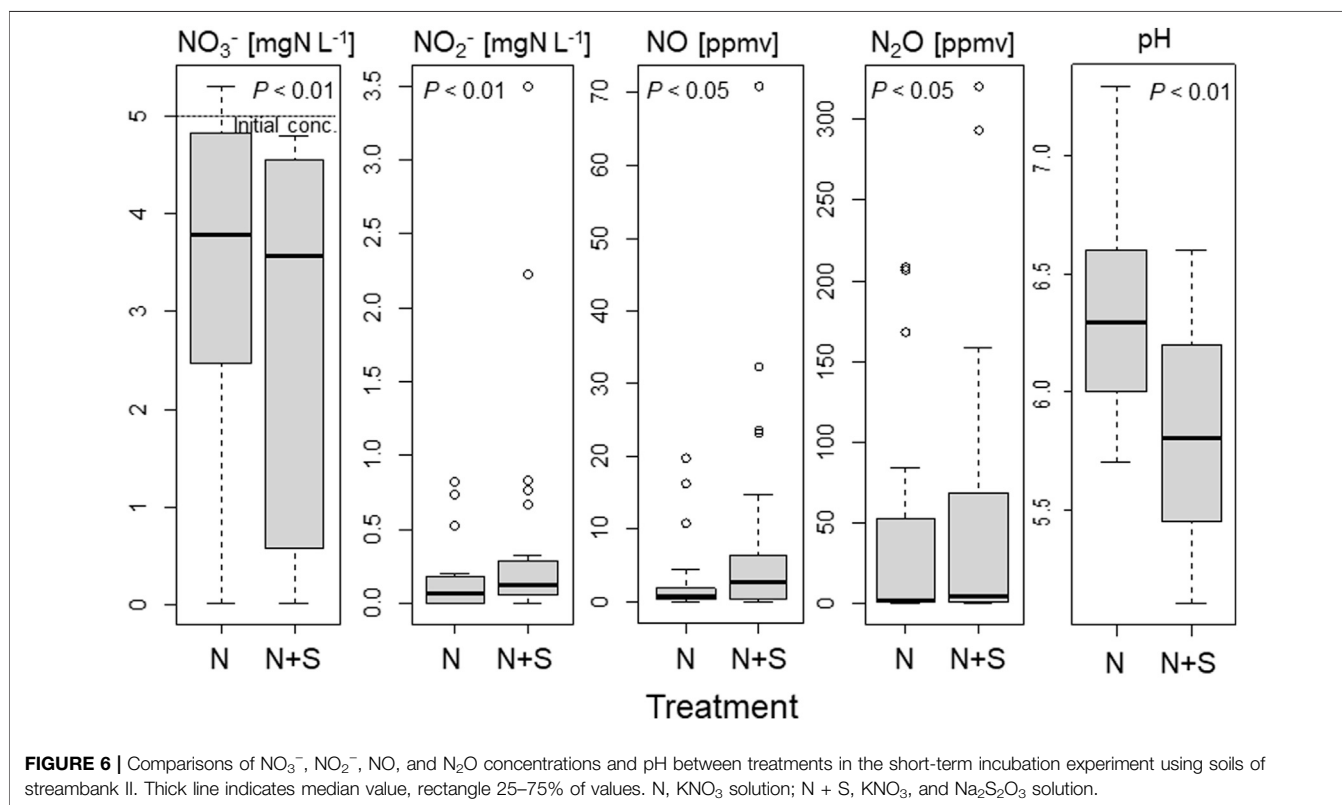
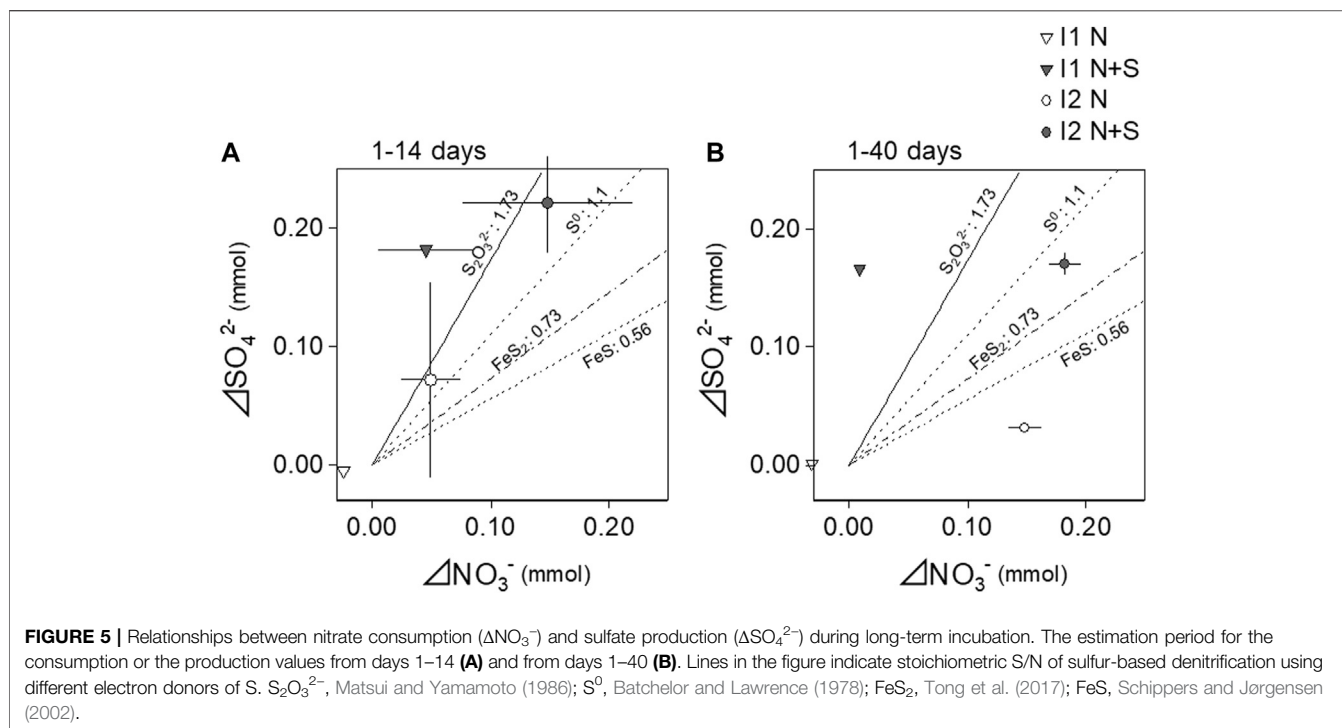
Bacterial Communities in the Soil

The following were considered to be sulfur-oxidizing bacteria (SOB) in this study [name (Genbank accession number)]; Bacterium ML2-86 (DQ145977.1), Bacterium PE03-7G2 (AB127721.1), *Halothiobacillus* sp. SS13102 (KM979607.1), Rhodocyclaceae bacterium FTL11 (DQ451827.1), *Sulfuricella denitrificans* skB26 (AP013066.1), *Sulfuricurvum kujiense* DSM 16994 (CP002355.1), *Sulfuricurvum kujiense* YK-3 (AB080644.1), *Sulfuritalea hydrogenivorans* sk43H (AP012547.1), Sulfur-oxidizing bacterium OAI12 (AF170423.1), *Thiobacillus aquaesulis* (U58019.1), *Thiobacillus denitrificans* strain AGR/IICT/15B (LN614387.1), *Thiobacillus thioparus* strain NZ (KC542801.1), *Thiomonas arsenivorans* strain b6 (AY950676.1), *Thiomonas* sp. Ynys3 (AF387303.1). The relative abundances of SOB in I2 during the long-term incubation experiment are plotted in Figure 8. The significant differences ($p < 0.05$) among treatments were detected in *S. denitrificans* strain skB26 and *S. kujiense*, although no significant differences were detected any pairs of the data groups. The main SOB in the soil was *S. denitrificans* strain

TABLE 2 | Nitrate consumption (ΔNO_3^-) and sulfate production (ΔSO_4^{2-}), and $\Delta SO_4^{2-}/\Delta NO_3^-$ of the different estimation periods during long-term incubation.

Period	Layer	Treatment	ΔNO_3^-		ΔSO_4^{2-}		$\Delta SO_4^{2-}/\Delta NO_3^-$	
			mmol		mmol			
1–14	I1	N	-0.025 (0.0032)	a	-0.0049 (0.00067)	A	0.20 (0.042)	a
	I1	N + S	0.045 (0.041)	a	0.18 (0.0036)	Bc	18 (26)	a
	I2	N	0.049 (0.026)	a	0.072 (0.083)	ab	2.2 (2.9)	a
	I2	N + S	0.15 (0.072)	b	0.22 (0.042)	c	2.1 (1.8)	a
1–40	I1	N	-0.032 (0.0026)	a	0.0015 (0.0027)	a	-0.0043 (0.080)	a
	I1	N + S	0.0090 (0.0043)	B	0.17 (0.0012)	c	22 (11)	b
	I2	N	0.15 (0.014)	C	0.032 (0.0048)	b	0.22 (0.045)	a
	I2	N + S	0.18 (0.014)	D	0.17 (0.0097)	c	0.94 (0.12)	a

Different letters indicate significant differences detected using One-way ANOVA followed by Bonferroni's test ($p < 0.05$).



skB26, which accounted for 55% of SOB and 0.04% of all sequences in the original soil before incubation (**Figure 8**, Ori). In the N + S treatment, *S. denitrificans* and *S. kujense*

strain YK-3 increased on day 10 (N + S₁₀), and the combined abundance of both sequences increased to 3.3% of all bacteria. On day 30, the abundance of SOB relative to bacteria in the N + S

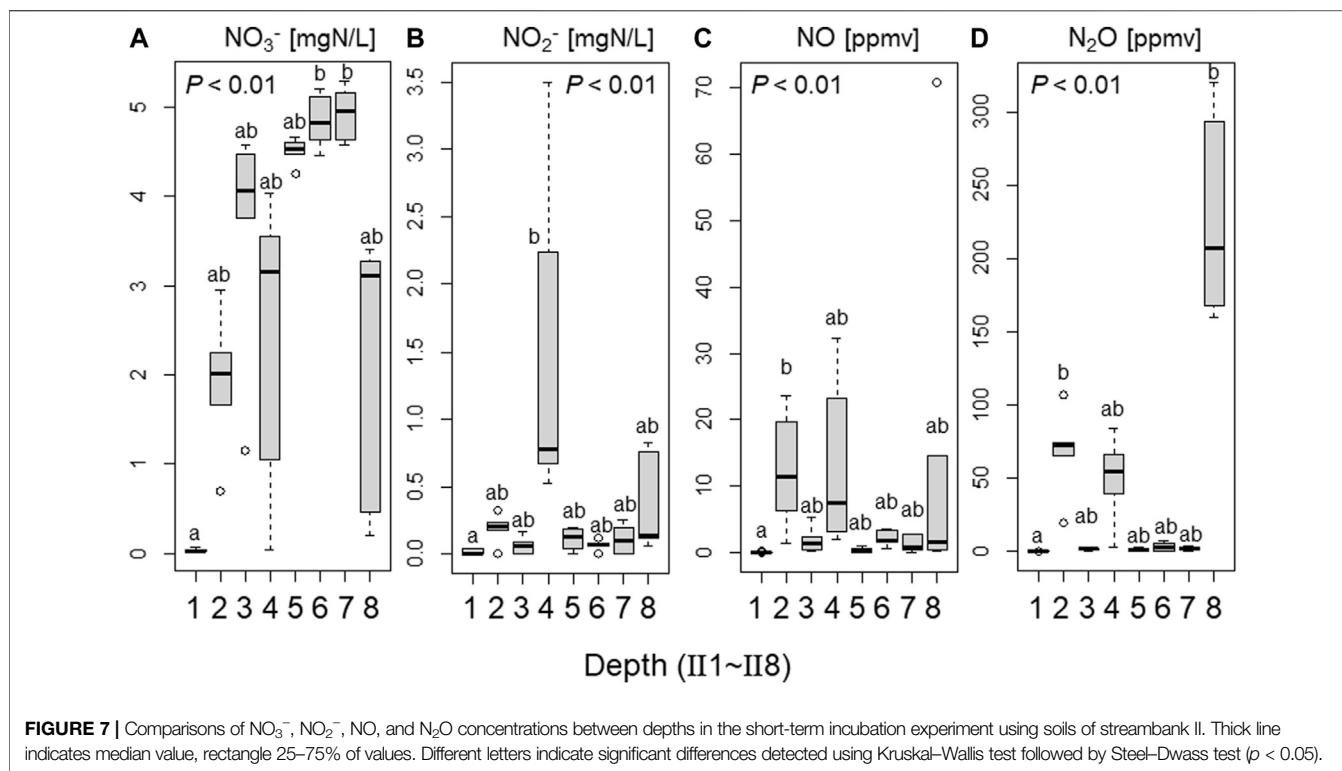


TABLE 3 | Summary data of the short-term incubation experiment using soils from streambank II. Values in parentheses indicate standard deviation ($n = 3$).

Layer	Treatment	pH	EC	NO_2d	NO_5d	N_2O_2d	N_2O_5d	NO ₃ ⁻	NO ₂ ⁻	SO ₄ ²⁻	NH ₄ ⁺
				mS m ⁻¹	Ppmv	ppmv	ppmv	ppmv	ppmv	mg N L ⁻¹	mg N L ⁻¹
II1	N	6.7 (0.1)	9.2 (0.6)	1.6 (0.6)	0.1 (0.0)	44 (33)	0.1 (0.1)	0.04 (0.02)	0 (0)	0.67 (0.07)	0.11 (0.01)
	N + S	6.5 (0.1)	12 (0.1)	1.4 (0.3)	0.1 (0.2)	43 (36)	0.1 (0.0)	0.02 (0.01)	0.03 (0.02)	6.7 (0.38)	0.12 (0.06)
II2	N	5.9 (0.1)	4.1 (0.9)	1.4 (0.3)	12 (10)	24 (10)	53 (28)	2.2 (0.67)	0.13 (0.11)	0.46 (0.05)	0.34 (0.01)
	N + S	5.4 (0.1)	7.3 (0.7)	1.6 (0.2)	12 (10)	12 (6.4)	84 (20)	1.7 (0.85)	0.25 (0.06)	6.0 (2.9)	0.30 (0.02)
II3	N	5.9 (0.1)	4.8 (0)	0.85 (0.3)	1.1 (0.9)	1.3 (0.0)	2.1 (0.5)	3.4 (2.0)	0.04 (0.03)	0.32 (0.21)	0.14 (0.03)
	N + S	5.2 (0.1)	10 (0.4)	1.1 (1.1)	2.7 (2.6)	0.8 (0.5)	1.8 (1.3)	4.0 (0.18)	0.09 (0.09)	8.6 (0.09)	0.10 (0.04)
II4	N	6.6 (0.1)	6.3 (0.4)	1.5 (0.9)	6.1 (4.1)	7.4 (2.8)	42 (41)	3.5 (0.55)	0.70 (0.15)	2.2 (0.53)	0.01 (0.005)
	N + S	6.3 (0.1)	12 (0.5)	1.5 (0.7)	19 (16)	4.1 (4.0)	58 (7.4)	1.5 (1.7)	2.1 (1.4)	11 (0.57)	0.01 (0.004)
II5	N	6.9 (0.4)	4.8 (0.4)	0.92 (0.6)	0.6 (0.4)	1.4 (0.4)	1.9 (0.7)	4.5 (0.21)	0.17 (0.04)	0.48 (0.04)	0.04 (0.003)
	N + S	5.8 (0.1)	9.9 (0.6)	0.12 (0.2)	0.1 (0.2)	0.3 (0.2)	0.5 (0.3)	4.5 (0.06)	0.05 (0.06)	8.9 (0.04)	0.004 (0.004)
II6	N	6.4 (0.1)	4.5 (0.4)	1.0 (1.1)	1.4 (0.6)	0.5 (0.2)	0.3 (0.2)	5.1 (0.11)	0.05 (0.04)	0.36 (0.02)	0.07 (0.01)
	N + S	5.8 (0.1)	10 (0.1)	2.1 (0.5)	2.9 (1.0)	1.1 (0.4)	6.1 (0.8)	4.6 (0.11)	0.09 (0.03)	8.9 (0.08)	0.10 (0.02)
II7	N	6.0 (0.1)	5.8 (0.2)	0.42 (0.4)	0.4 (0.4)	0.4 (0.2)	0.9 (0.6)	5.2 (0.01)	0.03 (0.05)	1.9 (0.06)	0.04 (0.01)
	N + S	5.6 (0.1)	10 (0.2)	0.44 (0.1)+	2.2 (1.0)	0.9 (0.1)	2.7 (0.6)	4.7 (0.11)	0.19 (0.07)	8.1 (0.07)	0.08 (0.01)
II8	N	6.3 (0.1)	11 (1.6)	3.4 (4.5)	0.9 (0.9)	33 (7.3)	190 (23)	3.3 (0.13)	0.11 (0.04)	10 (2.7)	0 (0)
	N + S	6.1 (0.1)	17 (6.1)	12 (9.4)	29 (37)	14 (14)	260 (87)	1.2 (1.6)	0.57 (0.39)	21 (7.7)	0.01 (0.02)

N, KNO_3 solution; N + S, KNO_3 and $\text{Na}_2\text{S}_2\text{O}_3$ solution.

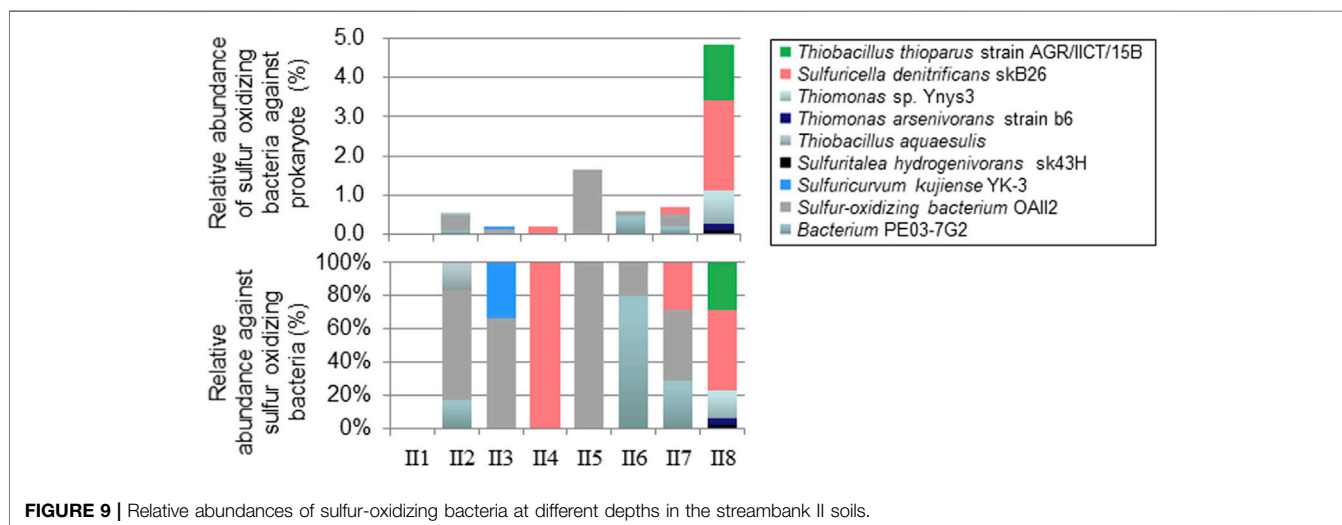
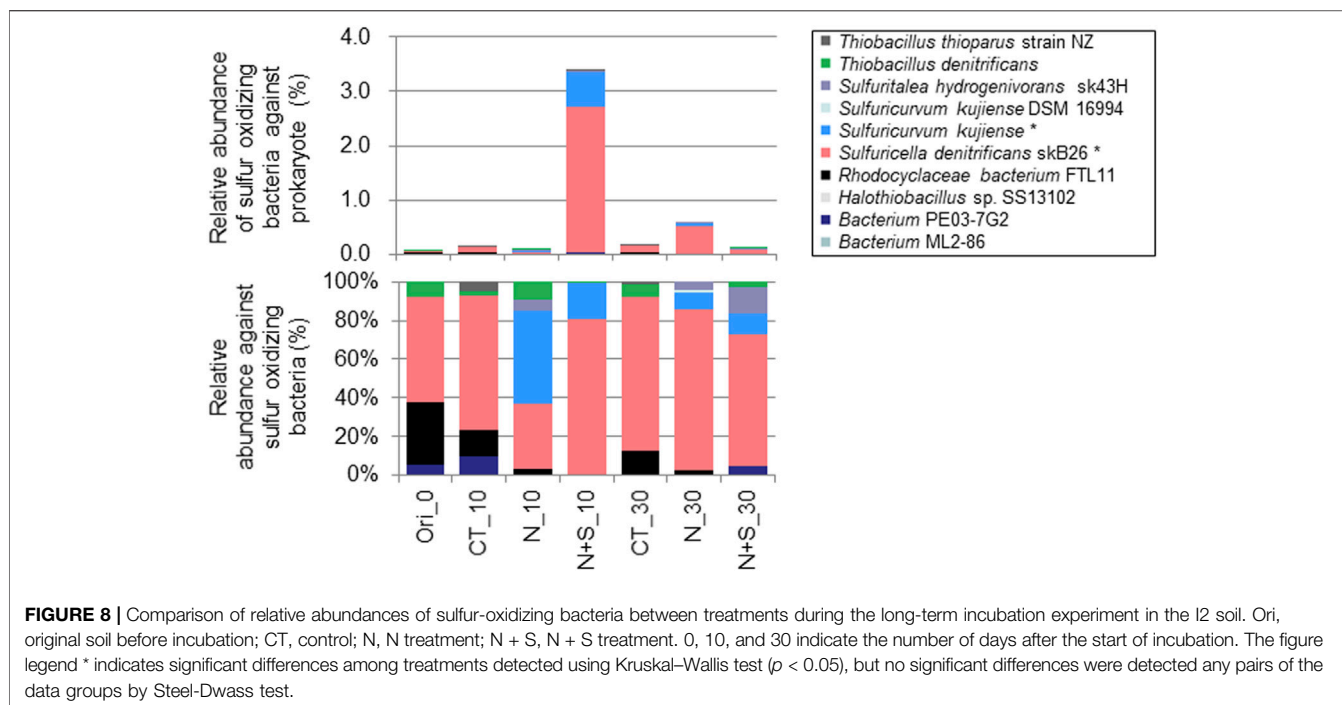
_2d, 2 days after the start of incubation; _5d, 5 days after the start of incubation.

treatment decreased, but rose to 0.6% in the N treatment. The vertical profiles of SOB relative abundance in the soils of streambank II are plotted in **Figure 9**. The relative abundance of SOB ranged from 0.0% in II1 to 4.8% in II8. *S. denitrificans* was detected in II4, II7, and II8. Similarly, *T. denitrificans* strain AGR/IICT/15B was detected only in II8. Of the SOBs detected in the streambank II soil layers, *S. denitrificans* (II4, II7, and II8), *T. denitrificans* (II8), and *S. hydrogenivorans* (II8) all occurred in the I2 soil (**Figures 8, 9**).

DISCUSSION

NO_3^- Reduction by Sulfur-Based Denitrification

Both the incubation experiments showed an NO_3^- reduction followed by increases in the NO_2^- , NO, and N_2O concentrations in some soils (**Figures 3, 7; Table 3**), indicating that denitrification had occurred. No accumulation of NH_4^+



indicated dissimilatory nitrate reduction to ammonium (DNRA) (Friedl et al., 2018) was not a major NO_3^- removal process. Especially in the long-term incubation experiment in I2, the successive peaks of NO_2^- , NO, and N_2O concentrations (Figure 4) strongly support the occurrence of biological denitrification (Tiedje 1994; Di Capua et al., 2019). The magnitude of the decrease of NO_3^- concentration indicates that the denitrification potential was higher in the soils of I2, II1, II2, II4, and II8 (Figures 3, 7). As discussed below, sulfur-based denitrification would be expected to occur predominantly in soils I2, II4, and II8, whereas other N-reduction processes such as heterotrophic denitrification could mostly take place in soils II1 and II2, depending on the

availability of electron donors and/or bacteria for denitrification.

Addition of thiosulfate significantly promoted reduction of NO_3^- and production of NO_2^- , NO, and N_2O (Figures 3, 6), indicating that sulfur-based denitrification had occurred. In I2 with N and N + S treatments, $\Delta\text{SO}_4^{2-}/\Delta\text{NO}_3^-$ for days 1–14 of incubation was large variation (2.1 ± 1.8 , Table 2) and crossed to the denitrification line using thiosulfate, S^0 , and FeS_2 as electron donors (Figure 5) with a decrease in pH (Figure 4), implying the occurrence of denitrification accompanying sulfur oxidation. II4 and II8 also exhibited relatively higher reduction of NO_3^- with added S (Table 3). These results indicate that sulfur-oxidizing bacteria in the soils had metabolized the added thiosulfate and

had promoted denitrification. In fact, *S. denitrificans* and *T. denitrificans*, which were relatively abundant in I2, I4, and I8, possess the ability to metabolize thiosulfate and can reduce NO_3^- (Kojima and Fukui, 2010; Shao et al., 2010). The increase in the relative proportions of *S. denitrificans* and *S. kujiense* on day 10 of I2 with N + S treatment (Figure 8) suggests that these bacteria were activated by the addition of thiosulfate. *S. kujiense*, which was detected in I2 and I3, also has the ability to reduce NO_3^- as the electron acceptor using thiosulfate (Kodama and Watanabe, 2004). Therefore, these bacteria are thought to be the key players in reduction of NO_3^- to NO_2^- by using thiosulfate.

The results of the long-term incubation also indicated that the phases controlling N reduction changed dramatically between the initial 14 day period and thereafter (Figures 4, 5 and Supplementary Figure S4). Sulfur-based denitrification may have been the predominant NO_3^- reduction process during the first 14 days in I2, and other N reduction processes such as heterotrophic denitrification may have occurred after day 14. The evidence supporting this conclusion is as follows: reduction of NO_3^- to NO_2^- accompanied by thiosulfate oxidation was clear during the first 14 days (Figure 4); the stoichiometric ratio of $\Delta\text{SO}_4^{2-}/\Delta\text{NO}_3^-$ was similar to the denitrification line using thiosulfate (Matsui and Yamamoto, 1986) during the first 14 days (Figure 5); and sulfur-oxidizing bacteria with NO_3^- reduction potential were detected and increased in relative abundance during this period (Figure 8). Chen et al. (2018) reported in a reactor study using solid S^0 as the electron donor for denitrification that the affinity of S^0 for NO_3^- was considerably higher than that for NO_2^- ; they also discussed the conversion of NO_3^- to NO_2^- , and of NO_2^- to N_2 , being performed by different microorganisms.

NO_2^- Accumulation and NO and N_2O Production

Temporal accumulation of NO_2^- was observed in this study (Figure 4; Table 3), as has also been demonstrated in previous bioreactor studies with added S (Moon et al., 2004; Chung et al., 2014; Liu et al., 2017; Chen et al., 2018). NO_2^- clearly accumulated during the first 10 days, particularly in I2 with S addition (Figure 4). Because the sum of NO_2^- and NO_3^- concentrations during this period was stable at approximately 8 mg N L^{-1} , which was equivalent to the added N concentration, NO_2^- reduction does not appear to have occurred, resulting in NO_2^- accumulation. Possible reasons for this are that the reduction of NO_2^- by sulfur-oxidizing bacteria is slower than the reduction of NO_3^- (Chung et al., 2014), and the higher affinity of sulfides for NO_3^- reduction than NO_2^- reduction, as discussed above. The S/N ratio in the added solution might also have been important for NO_2^- accumulation. Yamamoto-Ikemoto et al. (2000) observed accumulation of NO_2^- at added S/N (w/w) values of less than 4.35. Chung et al. (2014) reported that NO_2^- accumulation occurred at lower S/N ratios, possibly as a result of sulfide limitation, and complete denitrification required S/N of 5.1 (w/w). Liu et al. (2017) also observed NO_2^- accumulation at S/N values of 3.0 (w/w). In contrast, Qiu

et al. (2020) reported that, in short-term batch tests in a sulfur-based denitrification system, organic supplementation accelerated NO_2^- reduction, indicating that denitrifiers likely use organics preferentially over sulfur as the electron donors to reduce NO_2^- . In our study, relatively lower added S/N (w/w) in the long-term (2.5) and short-term (2.0) incubations and probable lower available organic C in the subsoil possibly caused the temporal NO_2^- accumulation. Other possible mechanisms for NO_2^- accumulation may have to do with the abilities of sulfur-oxidizing bacteria. *S. kujiense* (detected in I2 and I3) and *T. thioparus* (detected in I2 and I8; Figures 8, 9) can utilize thiosulfate as the electron donor and NO_3^- as the electron acceptor under anaerobic conditions, but can transfer NO_3^- to NO_2^- only (Kodama and Watanabe, 2004; Vaclavkova et al., 2015); thus, these bacteria, especially *S. kujiense* detected significant change among treatments (Figure 8), may also contribute to NO_2^- accumulation. Another possible reason for the NO_2^- peak may be that nitrite-reducing organisms start growing after the consumption of NO_3^- . In general, bacterial growth starts after substrate consumption (Maier and Pepper, 2014). Therefore, long-term incubation studies with higher substrate addition to subsoil which is expected to be low in bacteria, slower bacterial growth-rate may not be negligible for NO_2^- accumulation.

Our results also demonstrated that S addition to the soil markedly increased the production and temporal accumulation of NO and N_2O . Especially in I2, I4, and I8, increases in NO and N_2O concentrations were observed in association with S addition (Figures 4, 6, Table 3). This pattern may possibly result from the low added S/N ratio to the soils, the same reason as for the accumulation of NO_2^- . Lan et al. (2019) reported that a low S/N (w/w) ratio of one caused NO accumulation because competition for electrons caused incomplete denitrification (Velho et al., 2017; Pan et al., 2013). Another study reported that a high NO_2^- concentration (30 mg N L^{-1}) promoted NO accumulation (Castro-Barros et al., 2016). Our results also showed that N_2O concentration was higher with S addition, indicating enhanced N_2O production and accumulation (Figures 4, 6). Lan et al. (2019) also reported N_2O accumulation in a batch reactor experiment and discussed how higher NO_2^- levels can inhibit N_2O reductase activity and cause N_2O accumulation. In fact, a rapid reduction in N_2O was observed from day 26, when NO_2^- had almost disappeared (Figure 4). In contrast, Yang et al. (2016) revealed that N_2O accumulation at an S/N mass ratio of 5.0 was only 4.7% of that at 3.0 S/N, and found that the N_2O reduction rate was linearly proportional to the sulfide concentration at pH 7.0. Recent study reported that the electron distribution was significantly affected by sulfide loading rate, and the electron competition among nitrogen oxide reductases was intensified with the most electrons flowing towards NO_3^- reductase, and the least electrons towards N_2O reductase under decreased sulfide loading rate, which is more directly responsible for intermediates accumulation such as NO_2^- , NO, N_2O in sulfur-based denitrification process (Oberoi et al., 2021). Therefore, considering the use of lower S/N values in our study, it seems that sulfide was predominantly used for NO_3^- reduction, after which NO_2^- accumulated because of a sulfide limitation, and the

limited sulfide and accumulated NO_2^- might also have caused NO and N_2O accumulation (Figure 4). Future work should incorporate experiments matching the S/N values observed in natural soils.

Sulfur-Based Denitrification Using Inherent S in Subsoil in Marine Sedimentary Rock Regions

The inherent sulfide in the subsoils might be derived from the marine sedimentary rocks, which are highly enriched in total sulfur in the Akita region (Koma, 1992), and this enrichment is likely reflected in the high EOS content in streambed sediments (Figure 1, Hayakawa et al., 2020) and in the subsoils in this study. The optimum growth rate of *S. kujiense* occurs in low-intensity salty conditions (Kodama and Watanabe, 2004); this species was detected in I2. The EC in the subsoil of the study area was relatively high (Table 1), suggesting that the subsoil remains a relatively salty environment, reflecting the influence of marine sedimentary rocks and possibly providing suitable conditions for such bacteria.

The indigenous sulfides observed in this study would be useful electron donors for ecosystem-wide sulfur-based denitrification in the subsoil. EOS represents reduced sulfur such as pyrite (Murano et al., 2000), which has been reported to act as an electron donor for sulfur-based denitrification in streambed sediments (Hayakawa et al., 2013). Because subsoils I2, I4, and I8, in which signs of sulfur-based denitrification were detected, had a high EOS content (Table 1), EOS in those soils could have been the electron donor for denitrification by sulfur-oxidizing bacteria. In the N treatment of I2, thiosulfate was detected at low levels on day 1, the SO_4^{2-} concentration increased even without S addition (Figure 3; Table 2), and $\Delta\text{SO}_4^{2-}/\Delta\text{NO}_3^-$ was similar to the denitrification line using thiosulfate until day 14 (Figure 5). These results indicate that the original EOS in the I2 soil had provided available S as an electron donor for denitrification. In addition, the SO_4^{2-} concentrations in I4 and I8 without S addition (N treatment) were higher than those in other soil layers (Table 3), suggesting that the inherent sulfide had been oxidized to SO_4^{2-} and might have contributed to denitrification. However, detection of thiosulfate appears to be difficult, probably because the oxidation rate of inherent sulfide to thiosulfate is slow and the thiosulfate produced is rapidly oxidized to SO_4^{2-} (Figure 3). Therefore, thiosulfate was not detected during the short-term incubation. HS^- and S^0 other than thiosulfate can be also electron donors for sulfur-based denitrification (De Capua et al., 2019) and iron sulfides (FeS and FeS_2) can produce HS^- , S^0 and thiosulfate in their dissolution processes (Hu et al., 2020). X-ray powder diffraction analysis showed the diffraction patterns for I2, I4, and I8 soils were likely equivalent to pyrite (FeS_2) and pentlandite [$(\text{Fe}, \text{Ni})_9\text{S}_8$] (Supplementary Figure S5). Therefore, these iron sulfides might be electron donors for denitrification and the large variations of the stoichiometric ratios in I2 during days 1–14 (Figure 5 and Table 2) might have included the results of the oxidation of such iron sulfides from the indigenous sulfides in the catchment. Bacteria detected in this study subsoil also possess the

ability to metabolize S^0 (*S. denitrificans*, *T. denitrificans*, and *S. kujiense*) and HS^- (*T. denitrificans*), and can reduce NO_3^- (Kodama and Watanabe, 2004; Kojima and Fukui, 2010; Shao et al., 2010; De Capua et al., 2019; Cron et al., 2019).

In general, most NO_3^- is reduced by denitrifying heterotrophs rather than by chemoautotrophs such as sulfur-oxidizing bacteria because NO_3^- reduction by organic matter should thermodynamically precede reduction by sulfide (Postma et al., 1991). In the surface soil, heterotrophic denitrification was probably the dominant NO_3^- reduction process. In I11, little NO_3^- , NO_2^- , NO, and N_2O were detected after 5 days of incubation, but higher NO and N_2O concentrations were detected after 2 days (Table 3), indicating that denitrification had occurred rapidly. Because sulfur-oxidizing bacteria were not detected in I11 (Figure 9), NO_3^- was likely reduced by heterotrophs using relatively abundant organic carbon as the electron donor in the surface soil (Table 1). Therefore, when the conditions are suitable, denitrification will proceed more rapidly in surface soil than in the underlying soil. Carbon was also present in the subsoils (Table 1), but may be too old to be available for bacteria. Baker et al. (2012) suggested that pyrite was the main electron donor in subsoil because no significant decrease in organic C content was observed, likely because hardly decomposable organic C could not be exploited by heterotrophic microbes in the old sediments of the Jurassic Lincolnshire limestone. In contrast, Vaclavkova et al. (2014) found that sulfur-based denitrification co-occurred and accounted for approximately 30% of the net NO_3^- reduction, despite the presence of organic carbon, in a variety of Danish sediments. Cron et al. (2019) suggested that sulfur-oxidizing bacteria (*Sulfuricurvum kujiense*, also detected in this study) could use soluble organics to stabilize stores of bioavailable S^0 outside the cells. Recent bioreactor study reported key functional heterotrophic and autotrophic denitrifiers jointly contributed to high nitrogen removal efficiency by symbiotic relationships (Han et al., 2020). Although we did not measure organic C dynamics in this study, these symbiotic relationships may also occur in natural subsoil with lower available organic C in the study area.

The same denitrifying sulfur-oxidizing bacteria (*S. denitrificans*) were detected in the higher EOS subsoil layers I2, I4, I7, and I8 despite the different streambanks being located approximately 50 m apart (Figure 2), and beta diversity analysis shown that microbial communities in I4 and I8 were similar to those in I2 samples. (Supplementary Figure S3). *S. denitrificans* is a facultative anaerobic sulfur-oxidizing bacterium that was isolated from an anoxic layer (depth 40 m) from a freshwater lake in Japan (Kojima and Fukui, 2010). These results suggest that this bacterium is ubiquitous in the similar sulfide-containing layers in the catchments having higher EOS in riverbed sediments (Figure 1) and can contribute to NO_3^- reduction; in addition, because it is a freshwater bacterium, it is thought to have occurred in the soil only after the change from seawater to freshwater. However, the relative abundance of the bacterium was less than 5% of the total microbial community (Figures 8, 9). A previous

sludge reactor study also reported that *T. denitrificans* accounted for less than 5% of the entire microbial population by fluorescent *in situ* hybridization, despite clear NO_3^- reduction being observed (Dolejs et al., 2015). A small number of key players may be responsible for sulfur-based denitrification, especially in natural subsoils and sediments.

CONCLUSIONS

We detected multiple signs of sulfur-based denitrification in streambank subsoils in a headwater catchment underlain by marine sedimentary rock. Specifically, NO_3^- reduction accompanied by SO_4^{2-} production; a microbial stoichiometric $\Delta\text{SO}_4^{2-}/\Delta\text{NO}_3^-$ ratio indicative of denitrification using thiosulfate; accumulation of NO_2^- , NO , and N_2O ; and sulfur-oxidizing bacteria with the ability to reduce NO_3^- were detected in the subsoils with higher sulfide contents. The key player of sulfur-based denitrification in the subsoils appeared to be *S. denitrificans*, which is widespread and can exploit the inherent sulfide in those soils. These results revealed that the subsoils possess the potential for sulfur-based denitrification; therefore, sulfur-based denitrification in the subsoil is an important process for NO_3^- reduction and might control NO_3^- in the catchment. Further information on the quantity and three-dimensional distribution of sulfides and the functions associated with sulfur-oxidizing bacteria are required for better understanding and estimation of ecosystem-wide denitrification in sulfide-rich regions.

REFERENCES

- Adhikari, K., and Hartemink, A. E. (2016). Linking soils to ecosystem services - A global review. *Geoderma* 262, 101–111. doi:10.1016/j.geoderma.2015.08.009
- Baker, K. M., Bottrell, S. H., Hatfield, D., Mortimer, R. J. G., Newton, R. J., Odling, N. E., et al. (2012). Reactivity of pyrite and organic carbon as electron donors for biogeochemical processes in the fractured Jurassic Lincolnshire limestone aquifer, UK. *Chem. Geology*. 332–333, 26–31. doi:10.1016/j.chemgeo.2012.07.029
- Batchelor, B., and Lawrence, A. W. (1978). Autotrophic Denitrification Using Elemental Sulfur. *Journal (Water Pollution Control Federation)* 50, 1986–2001.
- Brunet, R. C., and Garcia-Gil, L. J. (1996). Sulfide-induced dissimilatory nitrate reduction to ammonia in anaerobic freshwater sediments. *FEMS Microbiol. Ecol.* 21, 131–138. doi:10.1016/0168-6496(96)00051-7
- Burgin, A. J., and Hamilton, S. K. (2007). Have we overemphasized the role of denitrification in aquatic ecosystems? A review of nitrate removal pathways. *Front. Ecol. Environ.* 5, 89–96. doi:10.1890/1540-9295(2007)5[89:hwotro]2.0.co;2
- Burgin, A. J., and Hamilton, S. K. (2008). NO_3^- --Driven SO_4^{2-} Production in Freshwater Ecosystems: Implications for N and S Cycling. *Ecosystems* 11, 908–922. doi:10.1007/s10021-008-9169-5
- Caporaso, J. G., Lauber, C. L., Walters, W. A., Berg-Lyons, D., Lozupone, C. A., Turnbaugh, P. J., et al. (2011). Global patterns of 16S rRNA diversity at a depth of millions of sequences per sample. *Proc. Natl. Acad. Sci.* 108, 4516–4522. doi:10.1073/pnas.1000801107
- Castro-Barros, C. M., Rodríguez-Caballero, A., Volcke, E. I. P., and Pijuan, M. (2016). Effect of nitrite on the N_2O and NO production on the nitrification of

DATA AVAILABILITY STATEMENT

The datasets presented in this study can be found in online repositories. The names of the repository/repositories and accession number(s) can be found below: <https://www.ddbj.nig.ac.jp/>, DRA011495.

AUTHOR CONTRIBUTIONS

AH: Conceptualization, methodology, investigation, writing-reviewing and editing of this study. HO: Investigation, analysis of soil and gas, and writing-original draft preparation. RA: Bacterial community analysis. HM: Methodology of soil analysis especially easily oxidizable sulfur. TI: Investigation and reviewing. TT: Supervision of this study.

FUNDING

This study was partly supported by a Grant-in-Aid for Research (B), No. 26281011, provided by the Japan Society for the Promotion of Science (JSPS).

SUPPLEMENTARY MATERIAL

The Supplementary Material for this article can be found online at: <https://www.frontiersin.org/articles/10.3389/fenvs.2021.664488/full#supplementary-material>.

low-strength ammonium wastewater. *Chem. Eng. J.* 287, 269–276. doi:10.1016/j.cej.2015.10.121

Chao, A., and Bunge, J. (2002). Estimating the number of species in a stochastic abundance model. *Biometrics* 58 (3), 531–539. doi:10.1111/j.0006-341x.2002.00531.x

Chen, F., Li, X., Gu, C., Huang, Y., and Yuan, Y. (2018). Selectivity control of nitrite and nitrate with the reaction of S_0 and achieved nitrite accumulation in the sulfur autotrophic denitrification process. *Bioresour. Tech.* 266, 211–219. doi:10.1016/j.biortech.2018.06.062

Chung, J., Amin, K., Kim, S., Yoon, S., Kwon, K., and Bae, W. (2014). Autotrophic denitrification of nitrate and nitrite using thiosulfate as an electron donor. *Water Res.* 58, 169–178. doi:10.1016/j.watres.2014.03.071

Craig, L., Bahr, J. M., and Roden, E. E. (2010). Localized zones of denitrification in a floodplain aquifer in southern Wisconsin, USA. *Hydrogeol. J.* 18, 1867–1879. doi:10.1007/s10040-010-0665-2

Cron, B., Henri, P., Chan, C. S., Macalady, J. L., and Cosmidis, J. (2019). Elemental Sulfur Formation by Sulfuric acid mediated by Extracellular Organic Compounds. *Front. Microbiol.* 10, 2710. doi:10.3389/fmicb.2019.02710

Di Capua, F., Pirozzi, F., Lens, P. N. L., and Esposito, G. (2019). Electron donors for autotrophic denitrification. *Chem. Eng. J.* 362, 922–937. doi:10.1016/j.cej.2019.01.069

Dolejs, P., Paclik, L., Maca, J., Pokorna, D., Zabranska, J., and Bartacek, J. (2015). Effect of S/N ratio on sulfide removal by autotrophic denitrification. *Appl. Microbiol. Biotechnol.* 99, 2383–2392. doi:10.1007/s00253-014-6140-6

Fang, Y., Gundersen, P., Vogt, R. D., Koba, K., Chen, F., Chen, X. Y., et al. (2011). Atmospheric deposition and leaching of nitrogen in Chinese forest ecosystems. *J. For. Res.* 16, 341–350. doi:10.1007/s10310-011-0267-4

Friedl, J., De Rosa, D., Rowlings, D. W., Grace, P. R., Müller, C., and Scheer, C. (2018). Dissimilatory nitrate reduction to ammonium (DNRA), not

- denitrification dominates nitrate reduction in subtropical pasture soils upon rewetting. *Soil Biol. Biochem.* 125, 340–349. doi:10.1016/j.soilbio.2018.07.024
- Galloway, J. N., and Cowling, E. B. (2002). Reactive Nitrogen and the World: 200 Years of Change. *AMBIO: A J. Hum. Environ.* 31, 64–71. doi:10.1579/0044-7447-31.2.64
- García-Gil, L. J., and Golterman, H. L. (1993). Kinetics of FeS-mediated denitrification in sediments from the Camargue (Rhône delta, southern France). *FEMS Microbiol. Ecol.* 13, 85–91. doi:10.1111/j.1574-6941.1993.tb00054.x
- Garrity, G. M., Bell, J. A., and Lilburn, T. (2005). “Genus *Thiobacillus*,” in *Bergey’s manual of systematic bacteriology*. Vol. 2, 2edn, Part B. Edited by G. M. Garrity 58–59. New York: Springer.
- Han, F., Zhang, M., Shang, H., Liu, Z., and Zhou, W. (2020). Microbial community succession, species interactions and metabolic pathways of sulfur-based autotrophic denitrification system in organic-limited nitrate wastewater. *Bioresour. Tech.* 315, 123826. doi:10.1016/j.biortech.2020.123826
- Hayakawa, A., Funaki, Y., Sudo, T., Asano, R., Murano, H., Watanabe, S., et al. (2020). Catchment topography and the distribution of electron donors for denitrification control the nitrate concentration in headwater streams of the Lake Hachiro watershed. *Soil Sci. Plant Nutr.* 66, 906–918. doi:10.1080/00380768.2020.1827292
- Hayakawa, A., Hatakeyama, M., Asano, R., Ishikawa, Y., and Hidaka, S. (2013). Nitrate reduction coupled with pyrite oxidation in the surface sediments of a sulfide-rich ecosystem. *J. Geophys. Res. Biogeosci.* 118, 639–649. doi:10.1002/jgrg.20060
- Horowitz, A. J., and Elrick, K. A. (2017). The use of bed sediments in water quality studies and monitoring programs. *Proc. IAHS* 375, 11–17. doi:10.5194/piahs-375-11-2017
- Hu, Y., Wu, G., Li, R., Xiao, L., and Zhan, X. (2020). Iron sulphides mediated autotrophic denitrification: An emerging bioprocess for nitrate pollution mitigation and sustainable wastewater treatment. *Water Res.* 179, 115914. doi:10.1016/j.watres.2020.115914
- Iribar, V., and Ábalos, B. (2011). The geochemical and isotopic record of evaporite recycling in spas and salterns of the Basque Cantabrian basin, Spain. *Appl. Geochem.* 26, 1315–1329. doi:10.1016/j.apgeochem.2011.05.005
- Japan Meteorological Agency (2013). Information of meteorological statistics. Accessed April 19 2013 <http://www.data.jma.go.jp/obd/stats/etrn/index.php>
- Juncher Jørgensen, C., Jacobsen, O. S., Elberling, B., and Aamand, J. (2009). Microbial oxidation of pyrite coupled to nitrate reduction in anoxic groundwater sediment. *Environ. Sci. Technol.* 43, 4851–4857. doi:10.1021/es803417s
- Kodama, Y., and Watanabe, K. (2004). *Sulfuricurvum kujiense* gen. nov., sp. nov., a facultatively anaerobic, chemolithoautotrophic, sulfur-oxidizing bacterium isolated from an underground crude-oil storage cavity. *Int. J. Syst. Evol. Microbiol.* 54, 2297–2300. doi:10.1099/ijs.0.63243-0
- Kojima, H., and Fukui, M. (2010). *Sulfuricella denitrificans* gen. nov., sp. nov., a sulfur-oxidizing autotroph isolated from a freshwater lake. *Int. J. Syst. Evol. Microbiol.* 60, 2862–2866. doi:10.1099/ijs.0.016980-0
- Koma, T. (1992). Studies on depositional environments from chemical components of sedimentary rocks-with special reference to sulfur abundance-. *Bull. Geol. Surv. Jpn.* 43, 473–548.
- Korom, S. F. (1992). Natural denitrification in the saturated zone: A review. *Water Resour. Res.* 28, 1657–1668. doi:10.1029/92wr00252
- Lan, L., Zhao, J., Wang, S., Li, X., Qiu, L., Liu, S., et al. (2019). NO and N₂O accumulation during nitrite-based sulfide-oxidizing autotrophic denitrification. *Bioresour. Tech. Rep.* 7, 100190. doi:10.1016/j.biteb.2019.100190
- Li, E., Deng, T., Yan, L., Zhou, J., He, Z., Deng, Y., et al. (2021). Elevated nitrate simplifies microbial community compositions and interactions in sulfide-rich river sediments. *Sci. Total Environ.* 750, 141513. doi:10.1016/j.scitotenv.2020.141513
- Lilburne, L., Eger, A., Mudge, P., Ausseil, A.-G., Stevenson, B., Herzig, A., et al. (2020). The Land Resource Circle: Supporting land-use decision making with an ecosystem-service-based framework of soil functions. *Geoderma* 363, 114134. doi:10.1016/j.geoderma.2019.114134
- Liu, C., Li, W., Li, X., Zhao, D., Ma, B., Wang, Y., et al. (2017). Nitrite accumulation in continuous-flow partial autotrophic denitrification reactor using sulfide as electron donor. *Bioresour. Tech.* 243, 1237–1240. doi:10.1016/j.biortech.2017.07.030
- Lovett, G. M., and Goodale, C. L. (2011). A New Conceptual Model of Nitrogen Saturation Based on Experimental Nitrogen Addition to an Oak Forest. *Ecosystems* 14, 615–631. doi:10.1007/s10021-011-9432-z
- Maier, R. M., and Pepper, I. L. (2014). “Chapter 3-Bacterial Growth,” in *Environmental Microbiology*. Editors I. L. Pepper, C. P. Gerba, and T. J. Gentry. Third Edition (Amsterdam: Elsevier), 37–56.
- Martínez-Santos, M., Lanzén, A., Unda-Calvo, J., Martín, I., Garbisu, C., and Ruiz-Romera, E. (2018). Treated and untreated wastewater effluents alter river sediment bacterial communities involved in nitrogen and sulphur cycling. *Sci. Total Environ.* 633, 1051–1061. doi:10.1016/j.scitotenv.2018.03.229
- Matsui, S., and Yamamoto, R. (1986). A New Method of Sulphur Denitrification for Sewage Treatment by a Fluidized Bed Reactor. *Water Sci. Tech.* 18, 355–362. doi:10.2166/wst.1986.0308
- Moon, H. S., Ahn, K.-H., Lee, S., Nam, K., and Kim, J. Y. (2004). Use of autotrophic sulfur-oxidizers to remove nitrate from bank filtrate in a permeable reactive barrier system. *Environ. Pollut.* 129, 499–507. doi:10.1016/j.envpol.2003.11.004
- Murano, H., Yamanaka, T., and Mizota, C. (2000). Origin of sulfides and associated sulfates in Neogene sediments along the Kitakami River basin from northeast Japan—Sulfur isotopic characterization and implications for land consolidation. *Pedologist* 44, 81–90. (in Japanese with English summary). doi:10.18920/pedologist.44.2_81
- Oberoi, A. S., Huang, H., Khanal, S. K., Sun, L., and Lu, H. (2021). Electron distribution in sulfur-driven autotrophic denitrification under different electron donor and acceptor feeding schemes. *Chem. Eng. J.* 404, 126486. doi:10.1016/j.ccej.2020.126486
- Pan, Y., Ye, L., and Yuan, Z. (2013). Effect of H₂S on N₂O Reduction and Accumulation during Denitrification by Methanol Utilizing Denitrifiers. *Environ. Sci. Technol.* 130710143655002, 130710143655002. doi:10.1021/es401632r
- Plugge, C. M., Zhang, W., Scholten, J. C. M., and Stams, A. J. M. (2011). Metabolic Flexibility of Sulfate-Reducing Bacteria. *Front. Microbio.* 2, 81. doi:10.3389/fmicb.2011.00081
- Postma, D., Boesen, C., Kristiansen, H., and Larsen, F. (1991). Nitrate Reduction in an Unconfined Sandy Aquifer: Water Chemistry, Reduction Processes, and Geochemical Modeling. *Water Resour. Res.* 27, 2027–2045. doi:10.1029/91WR00989
- Qian, J., Zhou, J., Zhang, Z., Liu, R., and Wang, Q. (2016). Biological Nitrogen Removal through Nitrification Coupled with Thiosulfate-Driven Denitrification. *Sci. Rep.* 6, 27502. doi:10.1038/srep27502
- Qiu, Y.-Y., Zhang, L., Mu, X., Li, G., Guan, X., Hong, J., et al. (2020). Overlooked pathways of denitrification in a sulfur-based denitrification system with organic supplementation. *Water Res.* 169, 115084. doi:10.1016/j.watres.2019.115084
- Roberts, A. P. (2015). Magnetic mineral diagenesis. *Earth-Science Rev.* 151, 1–47. doi:10.1016/j.earscirev.2015.09.010
- Schippers, A., and Jørgensen, B. B. (2002). Biogeochemistry of pyrite and iron sulfide oxidation in marine sediments. *Geochimica et Cosmochimica Acta* 66, 85–92. doi:10.1016/S0016-7037(01)00745-1
- Schwientek, M., Einsiedl, F., Stichler, W., Stögbauer, A., Strauss, H., and Maloszewski, P. (2008). Evidence for denitrification regulated by pyrite oxidation in a heterogeneous porous groundwater system. *Chem. Geology.* 255, 60–67. doi:10.1016/j.chemgeo.2008.06.005
- Shao, M.-F., Zhang, T., and Fang, H. H.-P. (2010). Sulfur-driven autotrophic denitrification: Diversity, biochemistry, and engineering applications. *Appl. Microbiol. Biotechnol.* 88, 1027–1042. doi:10.1007/s00253-010-2847-1
- Shiraishi, T. (1990). Holocene geologic development of the Hachiro-gata lagoon, Akita Prefecture, Northeast Honshu, Japan. *Mem. Geol. Soc. Jpn.* 36, 47–69. (in Japanese with English summary).
- Shiraishi, T., and Matoba, Y. (1992). Neogene paleogeography and paleoenvironment in Akita and Yamagata Prefectures, Japan Sea side of northeast Honshu, Japan. *Mem. Geol. Soc. Jpn.* 37, 39–51. (in Japanese with English summary).
- Straub, K. L., Benz, M., Schink, B., and Widdel, F. (1996). Anaerobic, nitrate-dependent microbial oxidation of ferrous iron. *Appl. Environ. Microbiol.* 62, 1458–1460. doi:10.1128/aem.62.4.1458-1460.1996
- Szynkiewicz, A., Johnson, A. P., and Pratt, L. M. (2012). Sulfur species and biosignatures in Sulphur Springs, Valles Caldera, New Mexico—Implications for Mars astrobiology. *Earth Planet. Sci. Lett.* 321–322, 1–13. doi:10.1016/j.epsl.2011.12.015
- Tiedje, J. M. (1994). “Denitrifiers,” in *Methods of Soil Analysis. Part 2. SSSA Book Ser. 5*. Editor R. W. Weaver (Madison: Soil Science Society of America), 245–257.

- Tong, S., Rodriguez-Gonzalez, L. C., Feng, C., and Ergas, S. J. (2017). Comparison of particulate pyrite autotrophic denitrification (PPAD) and sulfur oxidizing denitrification (SOD) for treatment of nitrified wastewater. *Water Sci. Tech.* 75, 239–246. doi:10.2166/wst.2016.502
- Torrentó, C., Cama, J., Urmeneta, J., Otero, N., and Soler, A. (2010). Denitrification of groundwater with pyrite and *Thiobacillus denitrificans*. *Chem. Geology*. 278, 80–91. doi:10.1016/j.chemgeo.2010.09.003
- Torrentó, C., Urmeneta, J., Otero, N., Soler, A., Viñas, M., and Cama, J. (2011). Enhanced denitrification in groundwater and sediments from a nitrate-contaminated aquifer after addition of pyrite. *Chem. Geology*. 287, 90–101. doi:10.1016/j.chemgeo.2011.06.002
- Vaclavkova, S., Jørgensen, C. J., Jacobsen, O. S., Aamand, J., and Elberling, B. (2014). The Importance of Microbial Iron Sulfide Oxidation for Nitrate Depletion in Anoxic Danish Sediments. *Aquat. Geochem.* 20, 419–435. doi:10.1007/s10498-014-9227-x
- Vaclavkova, S., Schultz-Jensen, N., Jacobsen, O. S., Elberling, B., and Aamand, J. (2015). Nitrate-Controlled Anaerobic Oxidation of Pyrite by *Thiobacillus* Cultures. *Geomicrobiology J.* 32, 412–419. doi:10.1080/01490451.2014.940633
- Velho, V. F., Magnus, B. S., Daudt, G. C., Xavier, J. A., Guimarães, L. B., and Costa, R. H. R. (2017). Effect of COD/N ratio on N₂O production during nitrogen removal by aerobic granular sludge. *Water Sci. Tech.* 76, 3452–3460. doi:10.2166/wst.2017.502
- Vitousek, P. M. (1997). Human Domination of Earth's Ecosystems. *Science* 277, 494–499. doi:10.1126/science.277.5325.494
- Wang, J.-J., Xu, L.-Z. -J., Huang, B.-C., Li, J., and Jin, R.-C. (2021). Multiple electron acceptor-mediated sulfur autotrophic denitrification: Nitrogen source competition, long-term performance and microbial community evolution. *Bioresour. Tech.* 329, 124918. doi:10.1016/j.biortech.2021.124918
- Wynn, J. G., Sumrall, J. B., and Onac, B. P. (2010). Sulfur isotopic composition and the source of dissolved sulfur species in thermo-mineral springs of the Cerna Valley, Romania. *Chem. Geology*. 271, 31–43. doi:10.1016/j.chemgeo.2009.12.009
- Yamamoto-Ikemoto, R., Komori, T., Nomuri, M., Ide, Y., and Matsukami, T. (2000). Nitrogen removal from hydroponic culture wastewater by autotrophic denitrification using thiosulfate. *Water Sci. Tech.* 42, 369–376. doi:10.2166/wst.2000.0405
- Yang, W., Zhao, Q., Lu, H., Ding, Z., Meng, L., and Chen, G.-H. (2016). Sulfide-driven autotrophic denitrification significantly reduces N₂O emissions. *Water Res.* 90, 176–184. doi:10.1016/j.watres.2015.12.032
- Yin, H., Yang, P., and Kong, M. (2019). Effects of nitrate dosing on the migration of reduced sulfur in black odorous river sediment and the influencing factors. *Chem. Eng. J.* 371, 516–523. doi:10.1016/j.cej.2019.04.095

Conflict of Interest: The authors declare that the research was conducted in the absence of any commercial or financial relationships that could be construed as a potential conflict of interest.

Publisher's Note: All claims expressed in this article are solely those of the authors and do not necessarily represent those of their affiliated organizations, or those of the publisher, the editors and the reviewers. Any product that may be evaluated in this article, or claim that may be made by its manufacturer, is not guaranteed or endorsed by the publisher.

Copyright © 2021 Hayakawa, Ota, Asano, Murano, Ishikawa and Takahashi. This is an open-access article distributed under the terms of the Creative Commons Attribution License (CC BY). The use, distribution or reproduction in other forums is permitted, provided the original author(s) and the copyright owner(s) are credited and that the original publication in this journal is cited, in accordance with accepted academic practice. No use, distribution or reproduction is permitted which does not comply with these terms.